



Contents lists available at ScienceDirect

Remote Sensing Applications: Society and Environment

journal homepage: www.elsevier.com/locate/rsase



Leveraging cloud-based computing and spatial modeling approaches for land surface temperature disparities in response to land cover change: Evidence from Pakistan

Mirza Waleed ^a, Muhammad Sajjad ^{b,*}

^a Department of Environmental Sciences, COMSATS University Islamabad, Pakistan

^b Department of Geography, Hong Kong Baptist University, Hong Kong Special Administrative Region

ARTICLE INFO

Keywords:

LULC
LST
Google earth engine
Geographic information systems
Remote sensing

ABSTRACT

Monitoring spatial-temporal land use land cover (LULC) patterns and related processes (e.g., land surface temperature—LST) is essential to sustainable development at local, regional, and national levels. In this context, the present study leverages cloud-computing-based Google Earth Engine and geo-information modelling techniques to provide spatial-temporal insights regarding LULC and LST over the past three decades (1990–2020) in Pakistan—a south Asian country with ~212 million people. Additionally, using Punjab province (the most populous and developed in Pakistan) as the study area, we empirically evaluate the association between several LULC types (i.e., built-up, forests, agriculture, rangeland, barren, and water) and LST. Our results show that due to the transition from rangeland and agriculture LULC to built-up areas (contributing 38 and 37%, respectively), ~250% increase is observed in the impervious surface in Punjab during 1990–2020. While the rapid urbanization has resulted in ~8.5 percent annual increase in built-up area during the study period, the highest percent change (~10.5%) occurred during the most recent decade (i.e., 2010–2020). This increase in built-up areas has led to LST rise with 1.4 °C increase in maximum annual LST in Punjab. In addition, among the evaluated top-20 cities, the most significant rise in LST is observed by Kasur city followed by Chiniot, Sheikhupura, Sahiwal, and Lahore—areas known for industrial development in Pakistan. While the results on LULC provide important references for rational and optimal utilization of land resource via policy implications, the association between LULC and LST ascertains why it is critical to design sustainable LULC planning and management practices for climate change mitigation and adaptation.

1. Introduction

Land is considered one of the most crucial resources sustaining human life. Changes in land use and land cover (LULC) in response to human activities over time result into several multi-scale (e.g., global, regional, and local) environmental consequences such as changes in surface energy balance and land surface temperature (LST). Land use and land cover are two different terminologies but are frequently used together. Land use refers to how land is utilized for various socio-economic prospects like agriculture and settlement among many others. On the other hand, land cover highlights biological or physical condition of terrestrial surfaces such as forests and water bodies etc. (Attri et al., 2015). LULC driving factors such as socio-economic activities, climatic, topographic, etc., are among the main reasons behind LULC changes around the world (Talukdar et al., 2020). Land-use change studies have gained im-

* Corresponding author.

E-mail address: mah.sajjad@hotmail.com (M. Sajjad).

portance in the recent decade due to a rise in environmental issues resulting from anthropogenic activities such as urbanization, deforestation, and transportation (X. P. Song et al., 2018). With the availability of freely accessible Landsat data, which host more than 40 years of multispectral satellite data archive, it is becoming much easier to monitor land use shifting trends cost-efficiently and at regular intervals (Ullah et al., 2019). Land change studies are also important as they address the issues related to Earth's energy balance and biogeochemical cycles, which directly affect local to regional climate and ecosystem services (Dewan et al., 2021a; Yohannes et al., 2021).

Land-use change studies play a crucial factor in defining the degradation rate of many environmental factors. Most of the time, land cover changes affect environmental phenomena such as UHI, surface temperature, biodiversity degradation, habitat loss, and high probabilities of flood events (Adnan et al., 2020; Hong et al., 2021). Most noticeably, land-use changes affect the microclimate of an area due to shifting land-use trends, i.e., from vegetative land to paved surfaces and thus increasing the surface temperature due to more heat absorption on bare surfaces. Thus, cities are at greater risk of facing harsh climates due to the UHI effect induced primarily due to such changes in land use patterns (Dewan et al., 2021a). The rapid urbanization has also resulted in more shift in rural to urban migration rate, which demands more basic life necessities such as shelter, food, hospitals, schools for education, etc. Thus, this facilitates more urban expansion, and surrounding habitats are severely affected (X. P. Song et al., 2018). Floods are another environmental factor that has been directly linked with changes in land use. The specific type of land cover determines the rate of water flow. Like in the case with paved surfaces, the water is not easily leached under the surface, and hence flash floods occur in higher precipitation receiving regions (Adnan et al., 2020).

Recent studies suggest that more than 40% of the global land area is changed to other land use types, and these changes are significantly linked to current and/or predicted environmental problems of the world such as the deterioration of natural systems those are providing essential services to sustain life on this planet (Borrelli et al., 2020; Magliocca et al., 2015; X.-P. Song et al., 2018; Wang et al., 2020; Winkler et al., 2021). One of the most visible human activities associated with these changes is urbanization, the most widely used predictor of LULC change over time and across space (Dilawar et al., 2021). During the past several decades, abrupt population influx and economic development have increased the pace of urbanization. It is predicted that ~70% of global population (2.5 billion) will be residing in urban regions in 2050 as compared to 55% in 2018, with Asia and Africa sharing 90% of the global population (Kundu and Pandey, 2020). This situation would further fasten the pace of urbanization, changing the Earth's terrestrial surface by large (Talukdar et al., 2020)—resulting in various challenges regarding climate and sustainable resources.

Among many others, one of the key issues related to urbanization is the response/sensitivity of climate indices to built-up areas (Amanollahi et al., 2016). Mapping LULC changes in the face of rapid urbanization and its associated influence on climatic conditions (e.g., LST) to comprehend climate related information is one of the foundational approaches for effective and sustainable planning (Saha et al., 2021). LULC changes from barren lands, agricultural areas, vegetation, and other rangelands to grey areas (impervious surfaces of built up infrastructure) as a consequence of urbanization influence local climate—increasing the magnitude of LST leading to the urban heat island (UHI) phenomenon—increase flood susceptibility, ecosystem degradation, and biodiversity loss. In a nutshell, LULC changes have serious consequences on natural systems along with compromising the comfortability of urban regions. Therefore, keeping track of LULC changes provides opportunities to understand its long-term association with LST, which is a strong climate change predictor (Das and Angadi, 2020). Additionally, assessment and systematic tracking of LULC changes provide crucial information regarding deforestation, growth in built-up areas, damage assessment, disaster monitoring, spatial planning, and land resources management. In this context, due to their easy to interpret nature, maps are essential tool for urban planners and decision-makers.

To map and evaluate LULC changes on spatial and temporal scales, remote sensing (RS) data and geographic information systems (GIS)-based techniques are preferred over conventional methods such as revenue records, statistical records (Abdullah et al., 2019; Attri et al., 2015; Vinayak et al., 2021). The integration of RS and GIS with other state-of-the-art modelling approaches improves the evaluation of LULC patterns in space and time (da Cunha et al., 2021). Additionally, RS and GIS-based methods are well known for their robust implementation, fast data acquisition, lower costs, and more detail and accurate results (Attri et al., 2015; Chachondhia et al., 2021). The change detection process analyzes multi-spatiotemporal datasets and quantifies LULC changes over time and space—answering questions related to “what”, “when”, and “where” in the context of long-term sustainability of the area of interest. Recent advances in this field suggest that the LULC classifications can be significantly improved by different spectral indices (Qu et al., 2021).

Spectral indices convert multi-spectral remotely sensed data into a single image, allowing a single pixel to be examined temporally (Xue and Su, 2017). Spectral indices are mostly preferred for analyzing multi-temporal changes due to the fact that they can enhance desired effect (like vegetation phenology changes) and reduce atmospheric and topographic noise (Hislop et al., 2018). The normalized difference vegetation index (NDVI) (Zhang et al., 2018), the enhanced vegetation index (EVI) (Jarchow et al., 2018), the soil adjusted vegetation index (SAVI) (Osgouei and Kaya, 2017), and the normalized difference water index (NDWI) (Özelkan, 2020) are the prominent spectral indices that are derived from the Landsat multi-spectral data. These spectral indices (NDVI, EVI, SAVI, NDWI) are preferred over others for their promising results in differentiating various land use types (Abdullah et al., 2019).

In the modern era, cloud computing has emerged since the last decade as a valuable and cost-effective platform for conducting studies on much larger scales (i.e., regional to global). For geospatial analyses, the Google Earth Engine (GEE) is one of the most dominant cloud computing platforms, which provides access to a petabyte of data catalogues through an interactive web-based application programming interface (Gorelick et al., 2017). With its flexible programming interface (JavaScript/Python), users can either use pre-defined models/algorithms or use their own for various computations. GEE data catalogue contains ~40 years of data (i.e., Landsat missions archives), opening doors for efficient time series analysis on a large geographical scale. Through its high-performance dedicated computing infrastructure, many computations that were previously achieved in hours or days are now completed in min-

utes or seconds (Kumar and Mutanga, 2018). In terms of land use classification, supervised and unsupervised classification are mostly used but in recent years Machine Learning (ML)-based classification is predominant. ML is a type of artificial intelligence (AI) and is based on the idea of “*learning from data*” (Jung et al., 2021). ML-based classifications are type of supervised classification that require training data. GEE provides many pre-defined ML-based algorithms (like Random Forest-RF, Support Vector Machines-SVM, Classification and Regression Tree-CART, etc.) that are set on defaults parameters but can be fine-tuned by users if needed (Gorelick et al., 2017). Among these several options, ML-based RF classifier is most widely used and has an upper hand due to its proven better and reliable results in exiting land use studies (Gumma et al., 2020; Shelestov et al., 2017).

Pakistan, a country in South Asia with ~212 million population (5th most populous), is particularly vulnerable to the impacts of climate change as the country is among the top-10 countries to be affected by global warming (Sajjad, 2021). This situation necessitates the comprehension of LULC changes and their association with LST to provide valuable references for effective planning in support of sustainable urbanization and climate adaptation. Previously, some studies have evaluated LULC changes and its association with climatic indices (i.e., LST) in some limited geographical areas of Pakistan. Among them, some studies (Amir et al., 2019; Dilawar et al., 2021; Hassan et al., 2016; Hussain and Karuppannan, 2021; Hussain et al., 2019) highlighted spatial-temporal dynamics of LULC changes but were limited in their geographical scale (i.e., focused on small and segmented areas comprising either only a few districts or a specific agro-ecological region). Also, some studies (Arshad et al., 2020; Cheema et al., 2020; Khana et al., 2020) used coarser-resolution datasets for LULC spatial-temporal evaluation, which do not provide promising results at local to regional scales (Afrin et al., 2019). Further, these existing studies do not provide up-to-date comprehensive literature on high-resolution LULC temporal changes. It is also important to note that there is no archive currently publicly available in Pakistan for higher resolution up-to-date long-term LULC changes. This lack of information hinders planning of natural resources, climate-related decision-making, urban planning, ecology monitoring, and act as a barrier for solution to numerous environmental challenges. Hence, there exists a significant knowledge gap to conduct comprehensive large-scale and spatially continuous LULC change assessment and its connection with climate indices, if any, in Pakistan at a higher resolution.

Hence, to overcome this gap, this study utilizes cloud computational capabilities of GEE, RF algorithm, tier-1 data of Landsat missions (Landsat-5 and Landsat-8) and spectral indices (NDVI, EVI, NDWI, SAVI) to provide higher resolution and long-term LULC and to evaluate the association between LST and several LULC types at district level in Punjab, Pakistan—the most populous and urbanized province in the country (sharing ~55% of total population). For this purpose, the satellite observation data between 1990 and 2020 are retrieved and processed systematically (see Section 2 for details). The results from this study will provide comprehensive information on multi-dimensional spatial-temporal LULC changes at provincial as well as district levels. This district-level information is particularly important as district is the administrative unit in Pakistan at which most of the planning and decision-making takes place. The up-to-date higher resolution LULC information provided through this study would be useful for several other computational purposes, such as multi-scaler climate modelling, LULC impact assessment on several phenomenon including ecosystem degradation and service change, hazard exposure/risk analysis, and urbanization as well as bio-diversity related issues. Additionally, while the LULC change assessment will progressively support sustainable urbanization in Pakistan, the results will also provide important references for resource management and climate adaptation in a more effective way, which might not be possible otherwise.

2. Methodology

2.1. Study area

As aforementioned, this study is primarily focused on Punjab province in Pakistan due to its huge population, high economic activity, and rapid urbanization process over the past few decades (Fig. 1). The study area extends from 27°N to 75°E and is 168.2 m above sea level. Punjab province has 9 divisions (administrative unit below province) which further consists of 36 total districts (administrative unit used in this study). Punjab province has an area of more than 205, 344 Km² having five major rivers (Jhelum, Chenab, Ravi, Sutlej, and Beas), which are further divided into ~ 3000 smaller channels (Imran et al., 2019). As a result, Punjab has a strong irrigation system which supports its agriculture production. (Siddiqui and Javid, 2019). About 55% of national income, 51% share of national exports, and ~70% of annual grain production in Pakistan is contributed by Punjab.¹ Six out of top ten cities in terms of gross domestic product (GDP) in Pakistan belong to Punjab making it an important economic hub. Furthermore, Punjab is home to 20 industrial zones attracting people from all other regions of the country (more information at <http://www.psic.gop.pk/>). This increasing population is also a major factor of rapid urbanization as the province has to cope with the increasing demand for land to accommodate the population influx. This urbanization-led infrastructural development significantly contributes towards LULC changes resulting in transition of other LULC types to built-up areas, which ultimately influences local climatic conditions such as disparities in LST. During this process, uninformed planning and expansion of built-up areas, particularly in major cities, have created many issues related to urbanization, ecosystem degradation, and environmental problems (Chen et al., 2019; Han, 2020; Sarkodie et al., 2020). To tackle such issues and to aid sustainable urban planning, it is integral to evaluate the spatio-temporal patterns and trends of different land-use types in Punjab and its associations with LST, if any.

2.2. Data acquisition and preparation

This study is conducted in several steps including data acquisition, LULC classification, change assessment, LST computation and evaluation, and identifying the association between different LULC types and LST. In general, the workflow is based on two major steps. The first step deals with data acquisition and employment of cloud-computing platform (Google Earth Engine) to identify sev-

¹ <https://www.usaid.gov/news-information/fact-sheets/provincial-fact-sheet-punjab>.

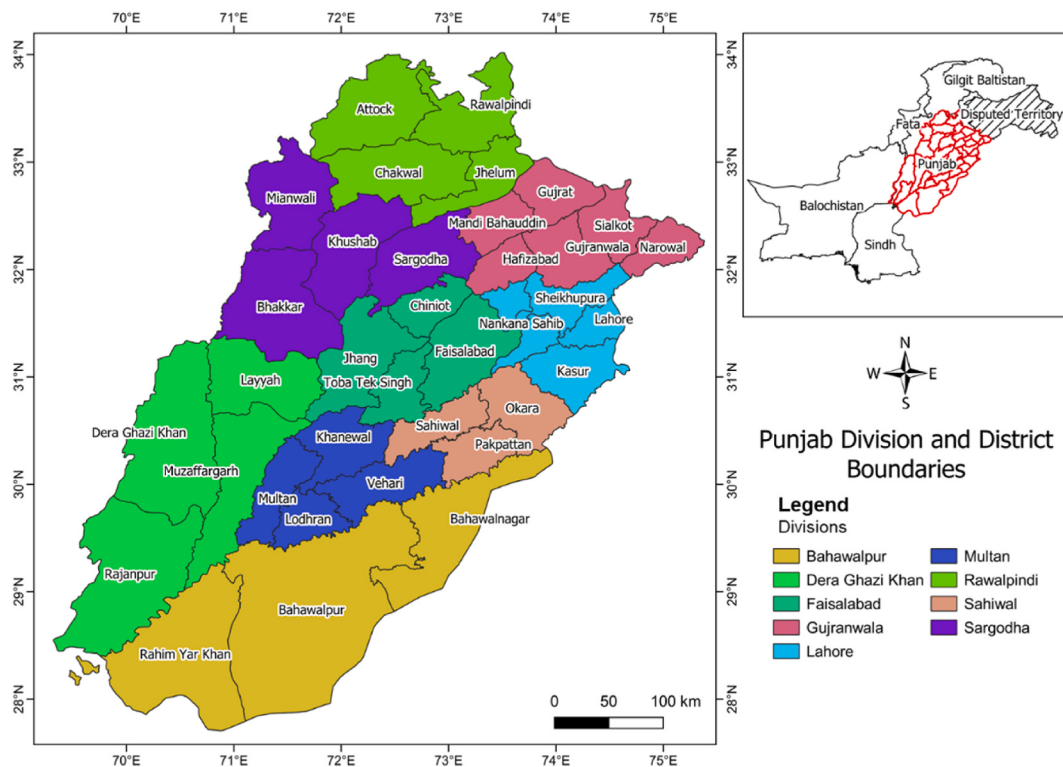


Fig. 1. Study area map.

eral LULC classes and retrieval of LST from the earth observation data for the entire study area. The second step consists of utilizing several geo-information modelling techniques to explore the spatial-temporal dynamics in LULC and LST along with evaluating the association between the both, if any. The overall workflow of the methodology adopted in this study is shown in Fig. 2. The data preparation stage starts with filtering the Landsat-5 Thematic Mapper (TM) tier-1 Surface Reflectance (SR) and Landsat-8 Operational Land Imager (OLI), and the Thermal Infrared Sensor (TIRS) tier-1 SR data from the GEE data catalogues in the form of image collection.

As LULC change is a slow process, we divide the analysis in four temporal periods (i.e., years 1990, 2000, 2010, and 2020). For the years 1990, 2000, and 2010 Landsat-5 TM tier-1 SR data was used, whereas for the year 2020 Landsat-8 OLI tier-1 SR data was used. Landsat-7 data was available for the year 2000 and 2010, but it was avoided because of scan-line error in it after 2003 (Yin et al., 2017). Except for the satellite observation-based data, we also use the vector data for provincial and district level boundaries as well as some network data (i.e., road networks). Details on all the data used in this study, their acquisition dates, and their source information are provided in Table 1. It is noted that atmospheric corrections were performed to avoid atmospheric disturbance like haze by identifying the darkest pixel value in each band and then by subtracting that value from each pixel (Chavez, 1988).

The Landsat path/row coverage scenes over Punjab are presented in Fig. 3. For the best pixel coverage and minimum cloud cover, average pixel values of first eight months from each year (i.e., 1990, 2000, 2010, and 2020) are filtered out and then clipped using the vector shapefile of Punjab province. The NDVI, NDBI, EVI, SAVI, and mNDWI are later calculated using the resultant clipped images and are added as separate bands. The details on these spectral indices are given in Table 2.

2.3. Training and LULC classification

Training and validation samples are collected using the Google Earth images and auxiliary data. Auxiliary data include Copernicus Global Land Cover Layer (CGLS-100), Moderate Resolution Imaging Spectroradiometer (MODIS) Land Cover data, Very High Resolution (VHR) Google Earth Images, and spectral indices including NDVI, NDBI, EVI, SAVI, and NDWI derived from Landsat-5 and Landsat-8 tier-1 SR data. Approximately 500–1500 training point samples are taken for each class using a stratified sampling approach. They are later split into a 70/30 ratio for training and validation, respectively. The 70% (~3500 points for each class) training samples are fed to RF classifier for supervised ML-based classification. In contrast, the remaining 30% (~1500) training samples are kept separate—for later use in validation process. For validation, those 30% samples are used to generate confusion matrix table of resultant maps. Confusion matrix also known as error matrix is a table that checks performance of classification model. Producer Accuracy (PA), User Accuracy (UA), Overall Accuracy (OA), F1-Score, and Kappa coefficient (K) are then derived from initial confusion matrix (AlBeladi and Muqaibel, 2018; Vinayak et al., 2021). The details of accuracy assessment techniques are given in Supplementary Table S1.

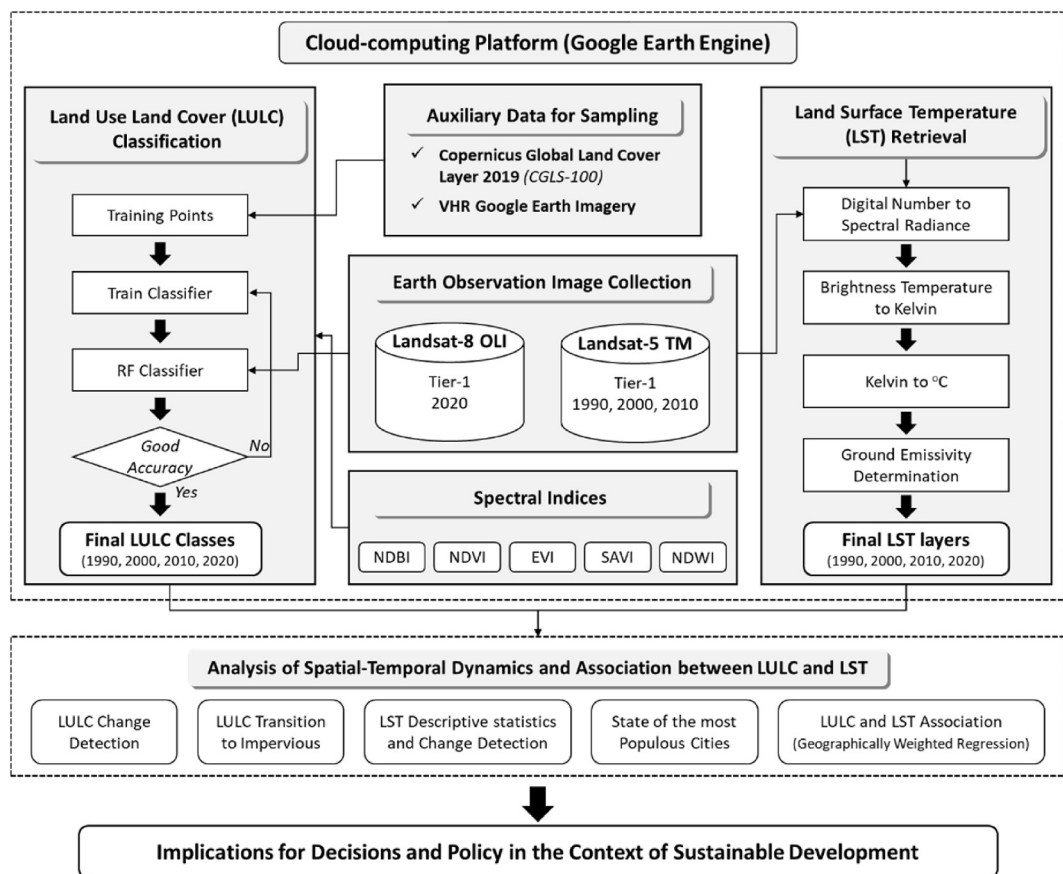


Fig. 2. Schematic of overall workflow to conduct this study.

Table 1

Detail on different datasets used in this study along with their sources.

Datasets	Resolution	Image Acquisition Date	Bands	Source
SRTM DEM	30 m	2007	['elevation']	https://lpdaac.usgs.gov/products/srtmgl1v003
Landsat-5 TM SR, TOA, Tier-1	30 m	1) Jan–Aug 1990 2) Jan–Aug 2000 3) Jan–Aug 2010	[1,2,3,4,5,7]	https://earthexplorer.usgs.gov
Landsat-8 OLI/TIRS SR, TOA, Tier-1	30 m	Jan–Aug 2020	[1,2,3,4,5,6,7]	https://earthexplorer.usgs.gov
Vector data on Punjab province and district boundaries (shapefiles)		2019		https://data.humdata.org/dataset/pakistan-administrative-level-0-1-2-and-3-boundary-polygons-lines-and-central-places
Punjab Roads		2020		https://data.humdata.org/dataset/hotosm_pak_roads

The RF classifier is used for the classification of different land use classes for each year (i.e., 1990, 2000, 2010, and 2020). Based on the existing literature, this study uses six different land use classes and their description is provided in Table 3. After tuning the RF classifier, optimal number of decision trees (n tree) are set to 120, which yields maximum accuracy. The obtained accuracies as described in Table 3 are used to test the performance of the RF classifier. Area for each class are calculated inside GEE using pixel-based approach (Xiong et al., 2017). The classified maps, confusion matrix table, and area estimation table are then exported locally from GEE. To analyze multi-year change in the area of each class, change detection is performed using QGIS software (available at <https://qgis.org/en/site/>), which is an open-source GIS software (Al-Rubkhi et al., 2017). Furthermore, Python 3 libraries such as NumPy, Pandas, Matplotlib, and Seaborn are used for statistical analyses and visualization.

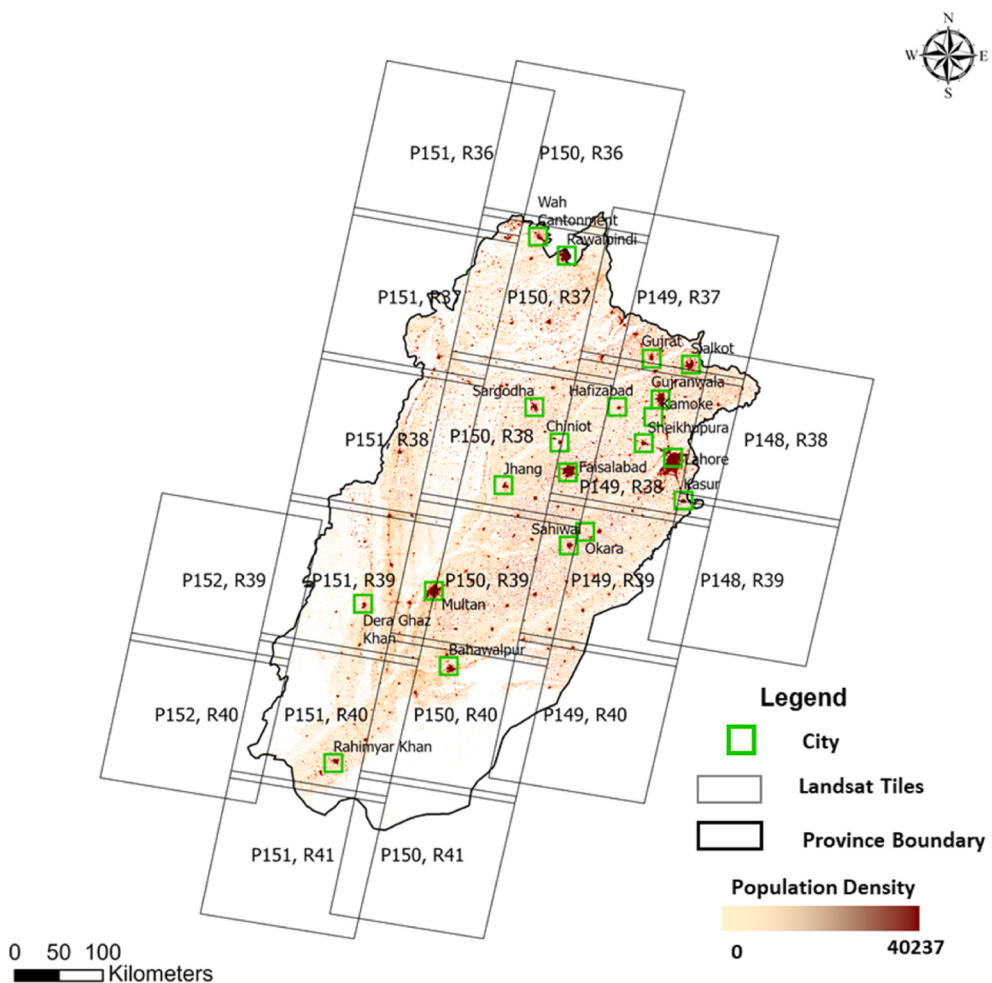


Fig. 3. Landsat Path/Row cover area. The base map presents the population density, and green boxes are the top-20 cities in the study area based on population. The "P" and "R" in the labels represent Path and Row of the Landsat satellite, respectively. (For interpretation of the references to color in this figure legend, the reader is referred to the Web version of this article.)

Table 2

Description on different spectral indices used in this study.

Index	Equation	Justification
EVI	$2.5 * (NIR - R) / (NIR + R + 1.0)$	Huete et al. (2002)
mNDWI	$(G - SWIR) / (G + SWIR)$	Xu (2006)
NDBI	$(SWIR - NIR) / (SWIR + NIR)$	Zha et al. (2003)
NDVI	$(NIR - Red) / (NIR + Red)$	Rouse et al. (1974)
SAVI	$(NIR - Red) / (NIR + Red + 0.5) * 1.5$	Huete (1988)

Note: NIR = Near InfraRed band, R = Red band, G = Green band, and SWIR = Shortwave InfraRed band of Landsat.

2.4. Evaluating LULC change

In general, change detection is the study of variations in state of an object with respect to change in a given time frame. In land use studies, change detection is of great importance as it not only shows statistics of gradual change over years but also visualizes spatial patterns among different land use classes over time. Among Pre- and Post-classifications techniques which are previously used for change analysis, post-Classification change detection is the most dominant and is widely used for most of land use studies (Abdullah et al., 2019).

Post-classification change analysis involves pixel-based comparison of classified maps of different times. This technique not only minimizes sensor, atmospheric, and environmental affect but also provides more in-depth view of land use transitions into various land use classes. Apart from that, this technique also evaluates change rates and magnitude of change that are important for individual class analysis. Previously many studies (Abdullah et al., 2019; Alawamy et al., 2020; Islam et al., 2018; Saputra and Lee, 2019; Zurqani et al., 2018) used post-classification change detection technique for evaluating land use spatio-temporal studies and acquired

Table 3

Land use types and their description.

Code	Land use class	Description
1	Built-up	Residential, commercial and services, industrial, transportation, roads, mixed urban, and other urban areas.
2	Forest	Dry tropical deciduous, Tropical wet evergreen, Alpine and Littoral forests
3	Barren	Exposed soils, construction sites, Deserts, little or no vegetation
4	Agriculture	Cultivated land, crop fields, fallow lands, and vegetable fields
5	Rangeland	Natural sparse vegetation, grasslands, shrublands, woodlands, tallgrass and shortgrass prairies, desert grasslands, savannas, chaparrals, steppes, and tundra
6	Water	Wetlands, inland water bodies, low-lying areas, marshy land, rills and gully, swamps, river networks, canals, active hydrological features

high accuracy. Therefore, post-classification comparison technique was used in this study for evaluating changes in LULC for each time period (i.e., 1990, 2000, 2010, and 2020). LULC classified maps are prepared for respective years and are then further analyzed in a workflow consisting of QGIS-based Semi-Automatic Classifier Plugin, Python modules (Pandas, Matplotlib, Seaborn), and Microsoft Excel. Resulting change maps and metrics are obtained and visualized to communicate the percent changes, magnitude of changes, and class transition. The details of change detecting algorithms used in this study are provided in [Supplementary Table S2](#).

2.5. Retrieving land surface temperature (LST)

The Top of atmospheric (TOA) Tier-1 data of Landsat-5 and 8 were filtered for summer months (from May till August) and mean of all values was taken individually for each year ([Li et al., 2020](#)). The resulting images for each year were then clipped with our study area shapefile. The resultant TOA images of Landsat-5 (i.e., 1990, 2000, and 2010) and Landsat-8 (2020) were then used to derive LST. Landsat-5 TM has one thermal band (band 6) whereas Landsat 8 OLI/TIRS has two thermal bands (band 10 and 11). To estimate LST, band 6 and band 10 of TM and TIRS, respectively, are used, whereas band 11 of TIRS is avoided because of the observed significant calibration issues as highlighted by the United States Geological Survey ([Avdan and Jovanovska, 2016](#)).

2.5.1. Converting digital numbers (DN) to spectral radiance (L_λ)

Thermal bands are used to convert Digital Numbers (DN) into spectral radiance (L_λ) using equations [\(1\)](#) and [\(2\)](#). The resulting top of atmospheric radiance (L_λ) is in watts/(m² × ster × μm) shown in equation [\(1\)](#).

$$L_\lambda = \left(\frac{L_{MAX} - L_{MIN}}{QCAL_{MAX} - QCAL_{MIN}} \right) \times (QCAL - QCAL_{MIN}) + L_{MIN} \quad \text{Eq. 1}$$

where L_{MAX} = maximum spectral radiances (15.600 for TM), L_{MIN} = minimum spectral radiances (1.238 for TM), $QCAL_{MAX}$ = maximum Digital Number (DN) value (255), $QCAL_{MIN}$ = minimum Digital Number (DN) value (1), $QCAL$ = Digital Number value of band 6.

The values of L_{MAX} , L_{MIN} , $QCAL_{MAX}$, and $QCAL_{MIN}$ are obtained from the metadata file attached with each Landsat images. For Landsat 8 OLI thermal band, top of atmospheric radiance (L_λ) is calculated using the following equation [\(2\)](#) provided by ([Rozenstein et al., 2014](#));

$$L_\lambda = M_L \times QCAL + A_L \quad \text{Eq. 2}$$

where M_L = multiplicative rescaling factor for specific band (0.0003342), $QCAL$ = digital numbers of band 10, and A_L = additive rescaling factor for specific band (0.1).

2.5.2. Converting spectral radiance (L_λ) to at-satellite brightness temperature

The TOA brightness temperature was calculated from spectral radiance using following equation [\(3\)](#):

$$T_B = \frac{K_2}{\ln \left(\frac{K_1}{L_\lambda} + 1 \right)} \quad \text{Eq. 3}$$

where T_B = at-satellite brightness temperature in Kelvin (K), L_λ = spectral radiance, K_1 and K_2 = calibrated constants depending on sensor. For Landsat-5 TM, the values of K_1 and K_2 are 607.76 and 1260.56, respectively. Whereas, for Landsat-8 OLI, the values of K_1 and K_2 are 774.89 and 1321.08, respectively ([Ihlen, 2019](#)).

2.6. Evaluating land surface temperature (LST) and its association with LULC

The at-satellite brightness temperature obtained from equation [\(3\)](#) also known as black body temperature, needs further corrections (spectral emissivity (ϵ)) to evaluate LST. Algorithm proposed by ([Artis and Carnahan, 1982](#)) is used to calculate emissivity corrected LST. The emissivity correction primarily depends on the category of land use and it is evaluated using Normalized Difference Vegetation Index (NDVI) per pixel values. The following equation [\(4\)](#) is used to evaluate emissivity corrected LST:

$$S_T = \frac{T_B}{1 + \left(\frac{\lambda \times T_B}{\rho} \right) \times \ln \epsilon} - 273.15 \quad \text{Eq. 4}$$

where S_T = land surface temperature in ($^{\circ}\text{C}$), T_B = at-satellite brightness temperature (K), λ = wavelength of emitted radiance ($11.5 \mu\text{m}$), $\rho = 1.438 \times 10^{-2} \text{ mK}$, ϵ = emissivity (ranges from 0.97 to 0.99).

Emissivity can be calculated by using equation (5) which is:

$$\epsilon = 0.004Pv + 0.986 \quad \text{Eq. 5}$$

where Pv = proportion of vegetation.

The proportion of vegetation Pv can be calculated using following equation (6);

$$Pv = \left(\frac{NDVI - NDVI_{min}}{NDVI_{max} - NDVI_{min}} \right)^2 \quad \text{Eq. 6}$$

where $NDVI$, $NDVI_{min}$, and $NDVI_{max}$ are per pixel value of NDVI, minimum NDVI, and maximum NDVI values, respectively.

It is noted that in this study, the values of Emissivity (ϵ) and Proportion of vegetation (Pv) are calculated by following the methodology adopted in (H. Imran et al., 2021).

To evaluate the association between LST and LULC types, many researchers have used the regression techniques (Dilawar et al., 2021; Saleem et al., 2020). Given the fact that both LST and LULC are spatially dynamic, it is better to use the regression technique that accounts for the spatial variations in the variables under consideration. Furthermore, while most of the linear approaches such as the ordinary least squares regression are global in nature, they are inadequate to comprehend the local spatial associations among the dependent and explanatory variables. Considering this, we use the geographically weighted regression (GWR) technique in this study to evaluate the relationship between several LULC types and LST, if any (Karimi et al., 2017). The general form of GWR for a given area of interest is as follows:

$$Y = \beta_0 + \beta_1 x_1 + \beta_2 x_2 + \dots + \beta_n x_n, \quad \text{Eq. 7}$$

where Y represents dependent variable (LST in this case) and $\beta_0, \beta_1, \beta_2, \dots, \beta_n$ are the slopes for each explanatory variable x_1, x_2, \dots, x_n . The explanatory variables used in this equation are the LULC types obtained from the classification of earth observations.

3. Results

3.1. Spatial-temporal evaluation of LULC (1990–2020)

Six primary classes including built-up, forest, barren, vegetation, rangeland, and water have been evaluated in Punjab to represent the dominant LULC. The overall distribution of all the LULC classes in Punjab is presented in Fig. 4. On a broader level the study area is dominantly covered by vegetation, barren areas, and rangeland types of LULC. While most of the vegetation is concentrated in the central to the eastern region of the study area (the regions in the floodplains of different rivers), the western regions primarily consist of barren and rangeland LULC throughout the study period (1990–2020). Three larger regions/zones are dominant in Punjab including vegetative area (central and eastern Punjab), rangeland (northwestern areas), and barren (southwestern and eastern borders). Notably, the visibility of intensifying built-up land (in red) can be easily observed during the study period presenting the growth of built-up land in Punjab between 1990 and 2020. The results show that the built-up area in Punjab is increased from 0.67 in 1990 to 2.35 million hectare (ha) in 2020. While the forest cover has been somehow steady during this period, there has been an increase in agricultural cover in 2020 as compared to 1990. Overall, Punjab has experienced a shrinkage in rangeland cover over the past three decades. These results on spatial-temporal LULC have important implications for land-use policy and natural resource management. Additionally, this relatively higher resolution data are particularly useful for several other purposes such as integration into climate or hydrological modelling. More detailed outcomes on spatial-temporal dynamics in the LULC are discussed in Section 3.3.

3.2. Evaluating the accuracy of LULC classification

One of the primary concerns of LULC classification is related to the reliability and accuracy of results. Given the fact that all the LULC estimation and classification techniques have some errors based on the method employed or the way of image acquisition, computing classification accuracies through different parameters become essential for reliability of the results (Ogunjobi et al., 2018). Fig. 5 represents the variations in the accuracy for each class and time step used in this study. It is evident that all the computed matrices (i.e., UA, PA, F1-score, OA, and K) for all the LULC types are approximately higher than 90%. These results show that the produced classification is reliable and can be used for further analyses. The minimum overall accuracy is estimated for the year 1990 (OA = 94.68) and the maximum is observed for 2020 (OA = 96.67). These results show that the classification presented in our study is much higher than the one reported by Saleem et al., (2020) (maximum reported OA value 88%), who conducted the analysis on three districts in Punjab recently. The base confusion matrices (also known as error matrix) for each year to compute all the typical aforementioned indices (i.e., UA, PA, F1-score, OA, and K) are provided in Figures 4b-4d—for 1990, 2000, 2010, and 2020, respectively—to represent the possible reasons for lower scores of certain accuracy indices along with helping readers preventing the confusion.

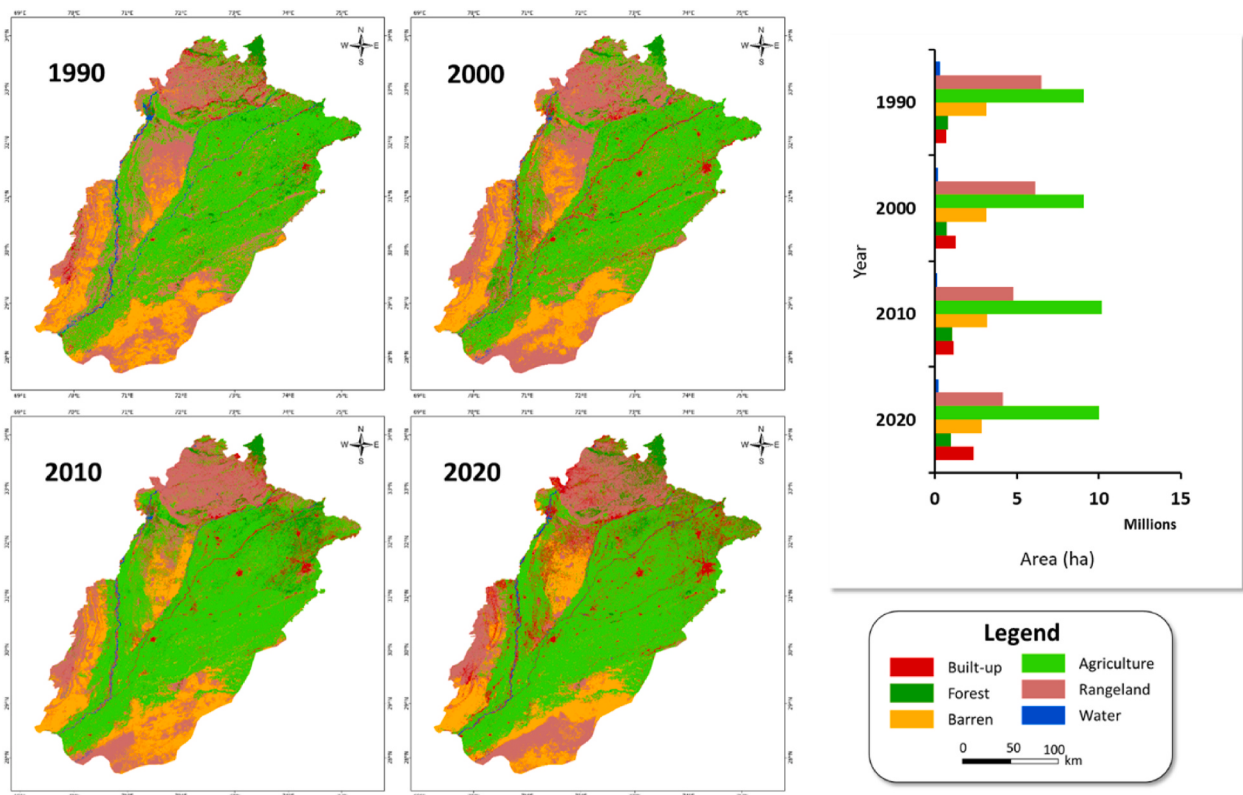


Fig. 4. Distribution of different LULC classes in the study area for the years 1990, 2000, 2010, and 2020. The bar chart represents the total area (ha) of each LULC class for different time periods between 1990 and 2020. Different colors in bar chart are consistent with the classification scheme presented in the map. It is noted that areas are calculated based on UTM zone 43 projected coordinate system in ArcGIS Pro software. (For interpretation of the references to color in this figure legend, the reader is referred to the Web version of this article.)

3.3. Multi-scale change detection in LULC (1990–2020)

The most dominant LULC types in 1990 are agriculture and rangeland (sharing 44% and 32% of total area, respectively) followed by barren land, forest, and built-up (Fig. 6). The largest reduction in rangeland is observed between the years 2000–2010, when the share of this LULC reduced from 30% in 2000 to 23% in 2010. It is observed that the built-up area has increased from ~3 of total area in Punjab to ~11 between 1990 and 2020 (Fig. 6a). Among top-20 cities according to population (Pakistan Population Census 2017), most of the regions experienced larger expansion during the earlier decade of the study period (i.e., Lahore, Faisalabad, Gujranwala, Multan, Jhang, Chiniot, and so on). This might be due to the fact that these areas are older cities. On the other hand, areas such as Rawalpindi, Rahim Yar Khan, Dera Ghazi Khan, Wah Cantonment, and Kamoke experienced larger built-up increase in recent two decades (i.e., between 2000 and 2020). This situation highlights the recent rapid urbanization in Punjab and increase in impervious surface areas.

The rapid urbanization process in Pakistan led to ~250% increase in built-up areas in Punjab over the past three decades (Table 4). Overall, the average percent change in built-up area in Punjab is observed at a rate of 8.32 percent per year during 1990–2020 with the highest percent change (10.43 percent per year) experienced in recent decade (i.e., between 2010 and 2020). Built-up area is followed by rangeland and water bodies in terms of percent change during past three decades (values 30.06 and 30.61, respectively). Among the forest, barren land, and agriculture LULC classes, barren land experienced loss of about 9.56%, whereas agriculture and forest show a gain (10.27% and 16.14%, respectively) during the study period.

Given the large percent change (~250%) in built-up area and its particular association with LST (Dilawar et al., 2021), we further evaluate the transition of different LULC classes to built-up area. The results on this assessment are presented in Fig. 7. It is observed that the largest contribution to built-up area between 1990 and 2020 is made by rangelands (38%) followed by agriculture land (37%). The transition of rangeland to built-up is observed mostly in western Punjab whereas, the agricultural transition is evident in the eastern Punjab. If this current trend of land transition is not sustainably managed, there is a high likelihood that along with facing the UHI phenomenon in Punjab, the agricultural sector might also experience several challenges such as land use conflicts or crop yield shrinkage.

3.4. Spatial-temporal assessment of LST and its association with LULC

The results from the LST estimation using earth observation data present interesting insights from a spatial-temporal perspective. On the basis of spatial distribution of LST, the southeastern regions in the study area observed the highest LST throughout the study

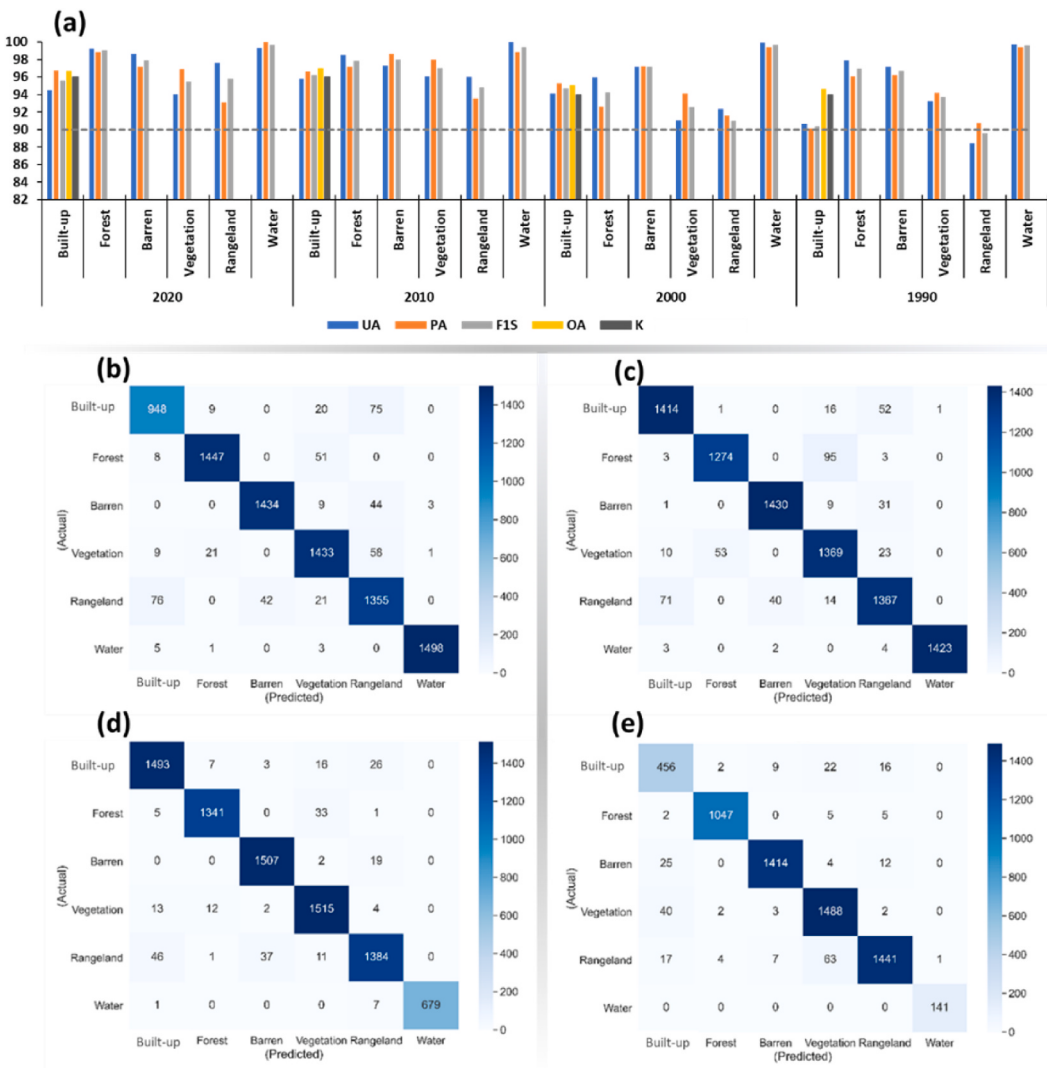


Fig. 5. Accuracy assessment of LULC classification. (a) shows percentage of user accuracy (UA), producer accuracy (PA), F1-score (F1S), overall accuracy (OA) and kappa coefficient (K). The dotted horizontal line in grey is for reference to 90% value. Heatmaps in (b)–(d) represent the confusion matrix on the relationship between actual and predicted pixels for 1990–2020, respectively.

period (190–2020) as presented by red shades in Fig. 8. This seems reasonable given that this highest LST region is mostly desert. Similarly, the region of Thar desert (central western Punjab—yellow shade in Fig. 8) and south western regions are also among the regions of comparatively higher LST. In general, there is an increasing spatial pattern in LST in the study area. At the provincial level, the highest max annual LST during the studied periods is observed in 2010 (48.18 °C). On the other hand, the minimum annual LST is observed for the year 2000 (19.88 °C). The largest spatial variation on the province scale is observed in 2010, followed by 2000, 2020, and 1990 (range values 26.74, 25.82, 24.25, and 23.32 °C, respectively). In the long-term, it is observed that the maximum observed LST has changed by 1.4 °C in Punjab during 1990–2020.

In addition to evaluating the LST at provincial scale and to provide preliminary references for local actions, we also analyze top-20 cities in terms of population according to the latest population census available at <https://www.pbs.gov.pk/>. The localized spatial heterogeneities of LST in these cities during the past three decades (1990–2020) are presented in the sub-sets of Fig. 8. The cities are arranged in descending population order (i.e., Lahore with the highest population and Hafizabad with the lowest among all). The spatial-temporal trends and patterns are evident in almost all of the cities, with relatively higher LST concentrated in central regions for most of the cities.

For 1990, the highest mean LST is observed for Bahawalpur (34.5 °C) followed by Dera Ghazi Khan and Rahim Yar Khan (Fig. 9a) —34 °C each. While the mean minimum LST is experienced by Gujrat, the highest maximum LST in 1990 is observed by Bahawalpur. The largest standard deviation and range is identified for Gujrat city, showing a large spatial disparity in the minimum and maximum LST throughout the city. Similarly, Bahawalpur also experienced the highest mean LST in 2000 (36 °C), showing an increase of 2 °C during 1990–2000. Rahim Yar Khan, Bahawalpur, and Sargodha are among the notable cities in 2010 with mean LST values of

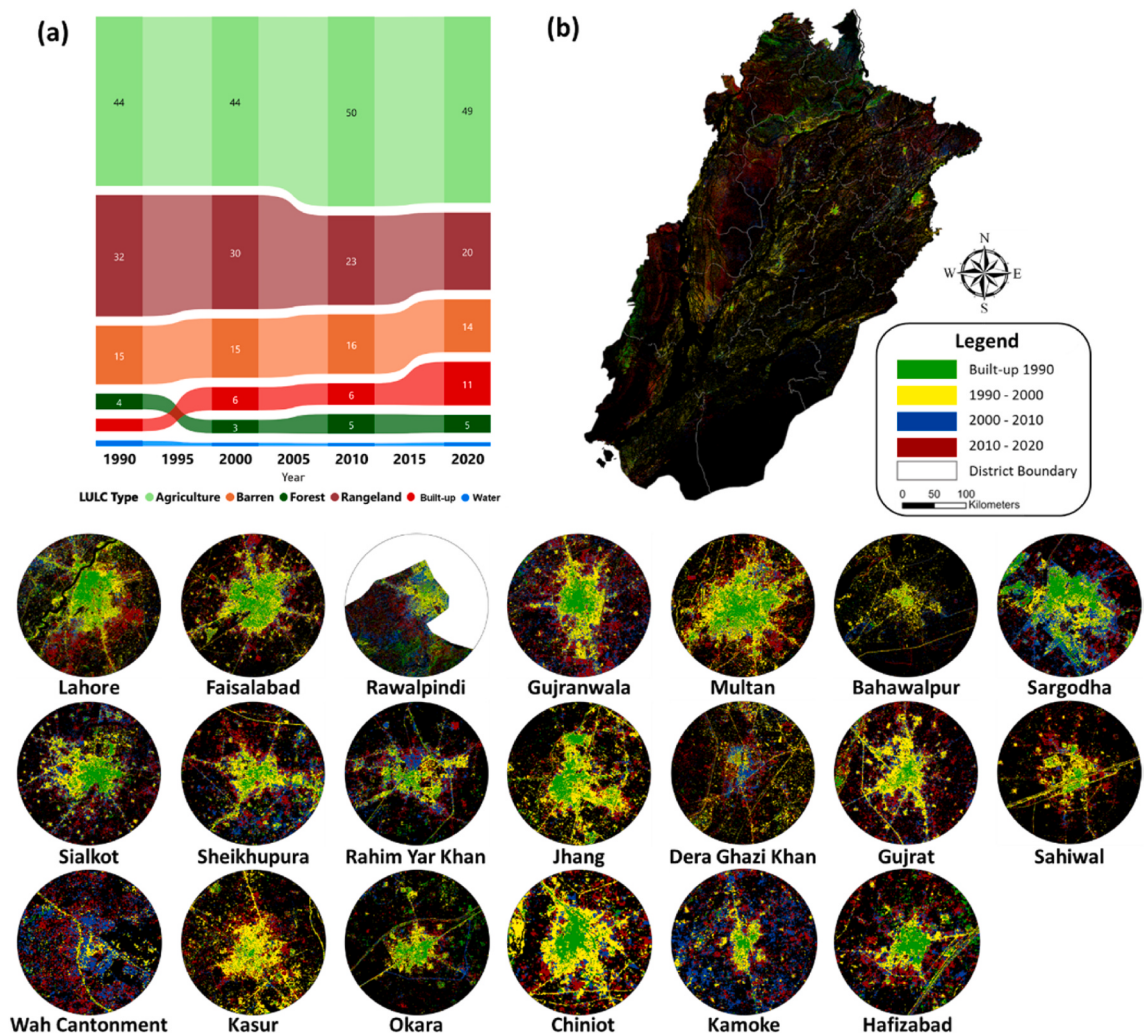


Fig. 6. Spatial-temporal dynamics of LULC in Punjab during 1990–2020. (a) share of different LULC types throughout the study period. (b) built-up area sprawl between 1990 and 2020. The inset maps (circles) show the top-20 countries in Punjab based on population (population data source: Pakistan Population Census 2017 available at www.pbs.gov.pk/). The arrangement of insets is according to high-low population (i.e., Lahore has high population and Hafizabad has relatively low. The maps are produced using ArcGIS Pro. Software.

Table 4

LULC percentage in Punjab as compared to total area and its change throughout the study period. The positive and negative values represent gain and loss in a certain LULC class, respectively.

LULC Class	% Area				1990–2000		2000–2010		2010–2020		1990–2020	
	2020	2010	2000	1990	Percentage Change (%)	Average Change						
Built-up	11.43	5.59	6.11	3.27	86.77	8.68	-8.39	-0.84	104.27	10.43	249.51	8.32
Forest	4.72	5.09	3.49	4.06	-13.96	-1.40	45.71	4.57	-7.36	-0.74	16.14	0.54
Barren	13.85	15.58	15.45	15.31	0.94	0.09	0.84	0.08	-11.15	-1.11	-9.56	-0.32
Agriculture	48.72	49.56	44.19	44.18	0.02	0.00	12.16	1.22	-1.70	-0.17	10.27	0.34
Rangeland	20.27	23.35	29.82	31.7	-5.94	-0.59	-21.68	-2.17	-13.21	-1.32	-36.06	-1.20
Water	1.02	0.82	0.94	1.47	-36.05	-3.61	-12.77	-1.28	24.39	2.44	-30.61	-1.02

38.5 °C, 37 °C, and 36.5 °C, respectively. In 2020, the mean, minimum, and maximum annual LST for Bahawalpur is also amongst the highest as compared to other cities. On the contrary, Gujrat is among the most noticeable cities due to its relatively largest local heterogeneity during 1990–2020, as reflected by the range and standard deviation values for all the periods (Fig. 9a–d).

To provide statistical evidence on the differences between the mean LST observed in different cities during 1990–2020, we further performed the analysis of variance (ANOVA) using different periods as different groups (four groups such as 1990, 2000, 2010, and

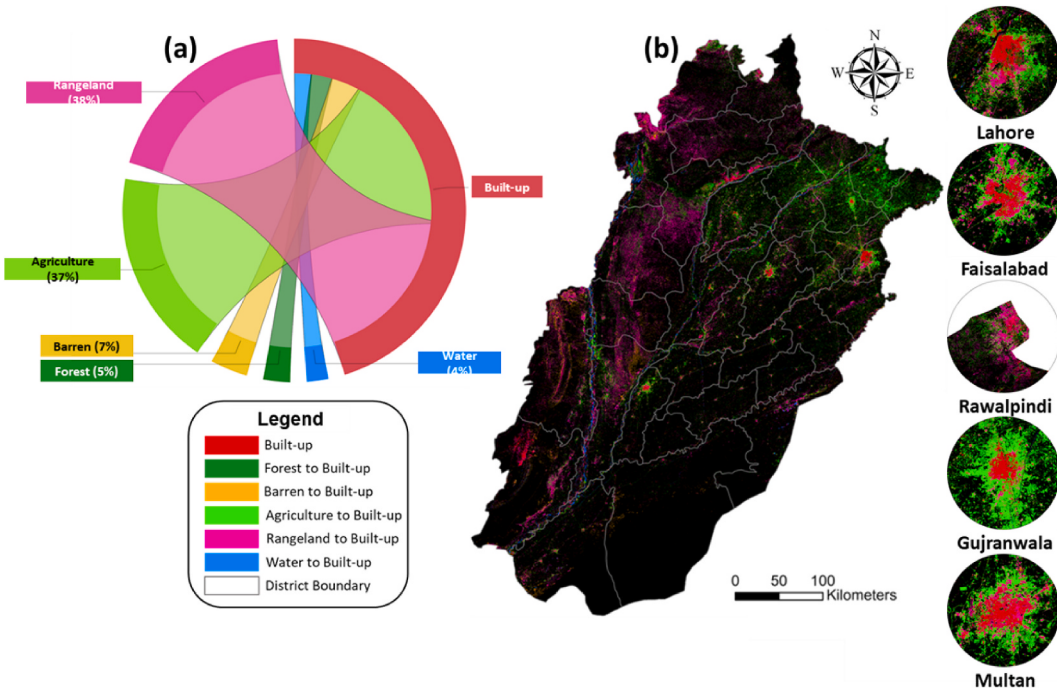


Fig. 7. LULC transition of different types to built-up areas between 1990 and 2020. (a) shows the percent contribution of each class to built-up areas, (b) represents the spatial references to what is changed to built-up between 1990 and 2020. The inset maps show the LULC transition of top-5 cities in Punjab according to population (population data source: Pakistan Population Census 2017 available at www.pbs.gov.pk/). The insets are arranged in higher to lower population order from top to bottom. The maps are produced using ArcGIS Pro Software.

2020). The results from ANOVA show statistically significant differences among the groups at $p < .05$. The resultant values of $p = .0004$ and $f\text{-ratio} = 6.88$ ascertain that the observed mean LST during different periods is statistically different. In addition, the pairwise comparisons based on the Tukey's HSD (Honestly Significant Difference) process show the significant differences among 1990–2000 (~86% confidence), 1990–2010 (99.9% confidence), 1990–2020 (91% confidence), 2000–2010 (92% confidence), and 2000–2020 (86% confidence) pairs. Whereas, the difference in 2010–2020 (the most recent decade) is insignificant ($p = .99$).

4. Discussion

It is a well-established fact that urbanization induced LULC changes are significantly associated with several challenges—with higher intensities in developing countries. On the one hand, many problems including but not limited to ecosystem degradation, threats to biodiversity, vegetation loss, and increase in impervious surfaces are linked to rapid urbanization (Qi et al., 2013). On the other hand, this LULC change is influencing climate at global, regional, and local scales—resulting in increased discomfort in urban areas (Kalnay and Cai, 2003). Moreover, rapid urbanization is increasing exposure to several hazards particularly floods and storm surges around the world (Hussein et al., 2020; Rahman et al., 2021; Zope et al., 2016). Hence, evaluating LULC changes through advance and integrated approaches such as provided in this study is of particular importance in terms of urban sustainable development. This assessment on LULC changes conducted across three decades (1990–2020) provides comprehensive insights related to “what” has changed and “where” in the study area—as presented in Figs. 4 and 6. Even though the rates of change are different, the increasing trends of built-up area found in our study (Table 4) are consistent with previous studies in Pakistan and beyond (Hu et al., 2019; H. M. Imran et al., 2021; Rosina et al., 2020; Saleem et al., 2020). Though no comparable studies are at hand for the observed variations in LULC due to higher resolution and large-scale assessment provided in this study, Hussain and Karuppannan (2021) noted an increase in the built-up areas in Khanewal (~201 percent change during 1980–2020)—consistent with our finding. Similarly, Shah et al. (2021) noted an increase in Islamabad's built-up area (~5.2% during 1979–2019), consistent with our evaluation. This increase in Punjab's built-up areas could be attributed to rapid urbanization process to accommodate the population influx the study area has witnessed in the past decades (i.e., ~50% increase during 1998–2017)—as reflected in the recent national census (Statistics, 2017).

Sustainable urban development prerequisites stable vegetative areas, which have the potential to reduce as well as maintain the thermal intensity in cities—particularly the denser built-up areas (Pramanik and Punia, 2020). Similarly, green areas (vegetation cover) in cities generate a cooling effect resulting into eco-environmental sustainability, and their absence potentially compromise comfort levels in urban areas (Amiri et al., 2009; Dewan et al., 2021b; Gunawardena et al., 2017). While rapid LULC changes could be associated with temporal undulations in UHI effect (Quan et al., 2016), the increased built-up area resulting in larger impermeable surfaces can contribute to reduced evapotranspiration (Wang et al., 2016)—having local and regional consequences. From this point

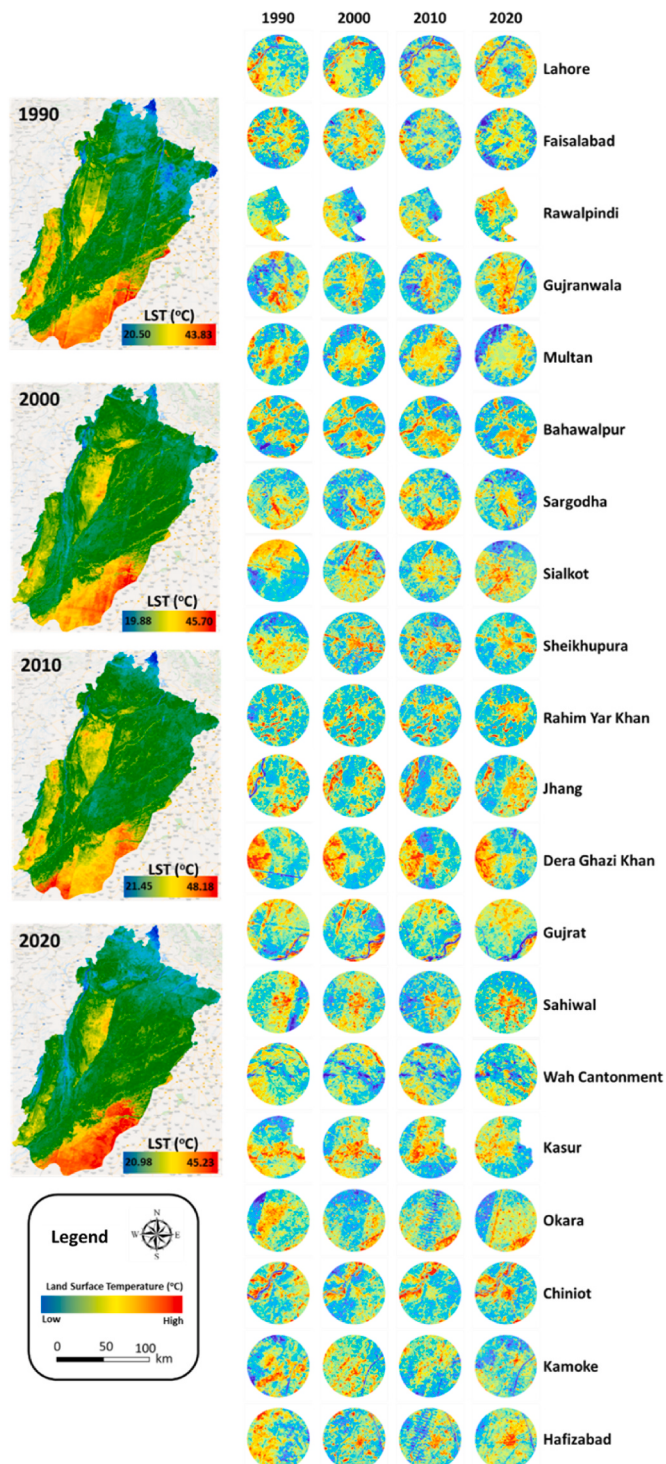


Fig. 8. Spatial-temporal dynamics of LST in Punjab during 1990–2020. The inset maps show the local distribution of LST in top-20 cities in Punjab according to population. Please see Fig. 3 for the exact locations of these cities. The values of LST are presented using two standard deviations where red and blue shades show high and low LST, respectively. The maps are produced using ArcGIS Pro Software. (For interpretation of the references to color in this figure legend, the reader is referred to the Web version of this article.)

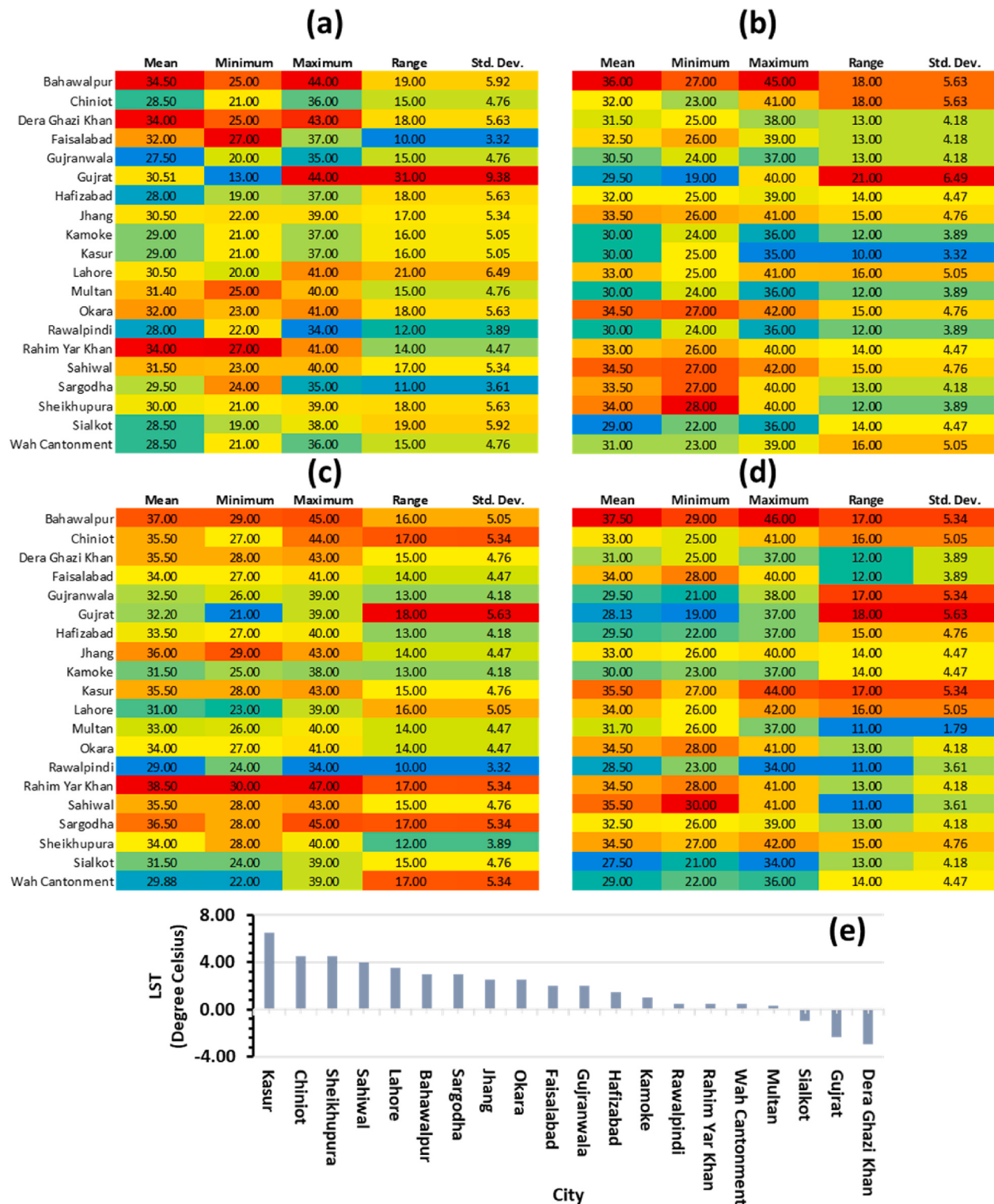


Fig. 9. Heat-charts of LST in top-20 cities in Punjab based on population. (a)–(d) represent summary statistics of LST for different time periods (i.e., 1990, 2000, 2010, and 2020, respectively), where red shades show the higher values and blue shades represent smaller LST values. (e) indicates the change in LST in top-20 cities during 1990–2020. (For interpretation of the references to color in this figure legend, the reader is referred to the Web version of this article.)

of view, the observed LULC modifications during the past three decades and an increase in impervious surface across the study area at the cost of vegetation cover (Fig. 7) should be a matter of serious concern for authorities. This transition of vegetation land cover to built-up is also consistent with (Hussain and Karuppantan, 2021; Majeed et al., 2021), and in contrast with Shah et al. (2021) who noted the higher contribution of barren land to built-up area in Islamabad during 1979–2019. This contradiction might be due to the different in scale (i.e., city scale in their study vs province level evaluation in this study).

As the dynamic geographic nature of LST, due to increase in impervious surface, in cities lead to UHI effect, it is essential to have insights regarding the spatial distribution of LST on local levels (i.e., cities) in order to design effective adaptation strategies (Simwanda et al., 2019). Urban areas of the developing world tend to have larger populations while being poorly equipped with the resources to cope with the consequences of urbanization process (Dewan et al., 2021a; Moretti, 2014). As a result, the rising temperature in cities (as reflected in Figs. 8 and 9) could have negative impacts on the livelihoods and health of millions (Huq, 2001). Hence, developing possible adaptation measures necessitates evaluation of spatial-temporal patterns and trends of urban warming (Ren et al., 2011), which is currently lacking for the cities in developing countries such as Pakistan and Bangladesh. In this context, the results from our study (Figs. 8 and 9) provide important preliminary references. For instance, the change in LST during 1990–2020 is higher in urbanizing mid-level cities such as Kasur, Chiniot, and Sheikhupura as compared with highly urbanized cities such as Lahore and Faisalabad. Hence, these urbanizing regions should not be overshadowed by the urbanized cities and should be provided with the due attention to take mitigation measures.

4.1. Fostering LULC and LST association-based informed planning

As LULC changes are significant in influencing regional climatic conditions, it is desirable to evaluate the association between LULC and LST for informed planning of urban areas. Hence, in order to evaluate the association between LULC and LST, we choose the most recent period (i.e., 2020) and aggregate the mean annual LST in 36 district-level boundaries in Punjab. Similarly, the LULC information is also aggregated in these district boundaries. To model the relationships, we aggregate the percent changes in the LST and all the LULC types for each district between 1990 and 2020. Later, using percent LST change (1990–2020) as dependent variable and the LULC types as explanatory variables, we first fit the individual models to evaluate the potential of each explanatory variable to explain the spatial variation in the LST (total six models). After that, an overall multivariate model is fitted to investigate the compound association between LULC types and the LST (Table 5).

Among the individual models, it is evident that largest variance is explained by agriculture 64%, $R^2 = 0.64$ followed by forest (63%, $R^2 = 0.63$) and urban models (61%, $R^2 = 0.61$). These outcomes are expected as all of these LULC play significant role to influence the LST in a given area (Dewan et al., 2021a; Ejiajha et al., 2020; H. M. Imran et al., 2021). On the other hand, the individual models based on barren, water, and rangeland perform poorly as reflected by their goodness-of-fit values (R^2 values of 0.29, 0.49, and 0.38, respectively). Moreover, the larger Akaike Information Criterion (AIC) value also represent the poor performance of rangeland and barren models (AIC values 234.47 and 235.18, respectively). For the multivariate model, initially, all the LULC types are selected as the explanatory variables. However, there exist a multicollinearity among the variables, which hinders the model running (more details at <https://bit.ly/3igr7pY>). To resolve this issue, the number of explanatory variables are reduced and several multivariate models are tested comparing them based on the goodness-of-fit and AIC values.

The most optimal model is achieved using the urban, agriculture, and rangeland LULC types as it shows $R^2 = 0.70$ and AIC = 220.64. This result shows that the multivariate model is able to explain 70% of variance in the dependent variable (LST in our case) in the study area. Local R^2 value for each district is mapped to show the spatially relative performance of this model (Fig. 10). The lowest local R^2 is observed for the eastern districts (55–60% variance explained). On the other hand, the central and south westerns districts have the highest local R^2 values (77–82% variance explained). This shows that even with the lowest goodness-of-fit value, the model performs reliably good. The reason behind this geographical disparity in local model performance could be the complexity of LULC in different regions. For instance, it is evident that most of the urban areas are concentrated in eastern and northern regions of the study area making the LULC more complex, and hence, the relatively lower goodness-of-fit is observed. On the contrary, the LULC is not that complex in the regions where the model performance is relatively higher. This situation highlights the need for scaling down to major urban regions and model these associations at higher levels to provide further insights in this regard. The results provided here (Figs. 4 and 6–8) are useful for such prioritization of regions to scale-down the areas for future assessments.

Table 5

Results from the Geographically Weighted Regression models. The individual models are arranged in descending order based on the goodness-of-fit value.

Model	Explanatory Variable[s]	Goodness-of-fit (R^2)	AIC
Individual Models	Agriculture	0.64	227.86
	Forest	0.63	228.55
	Urban	0.61	216.24
	Water	0.49	226.14
	Rangeland	0.38	234.47
	Barren	0.29	235.18
Multivariate model	Urban, Agriculture, Rangeland	0.70	220.64

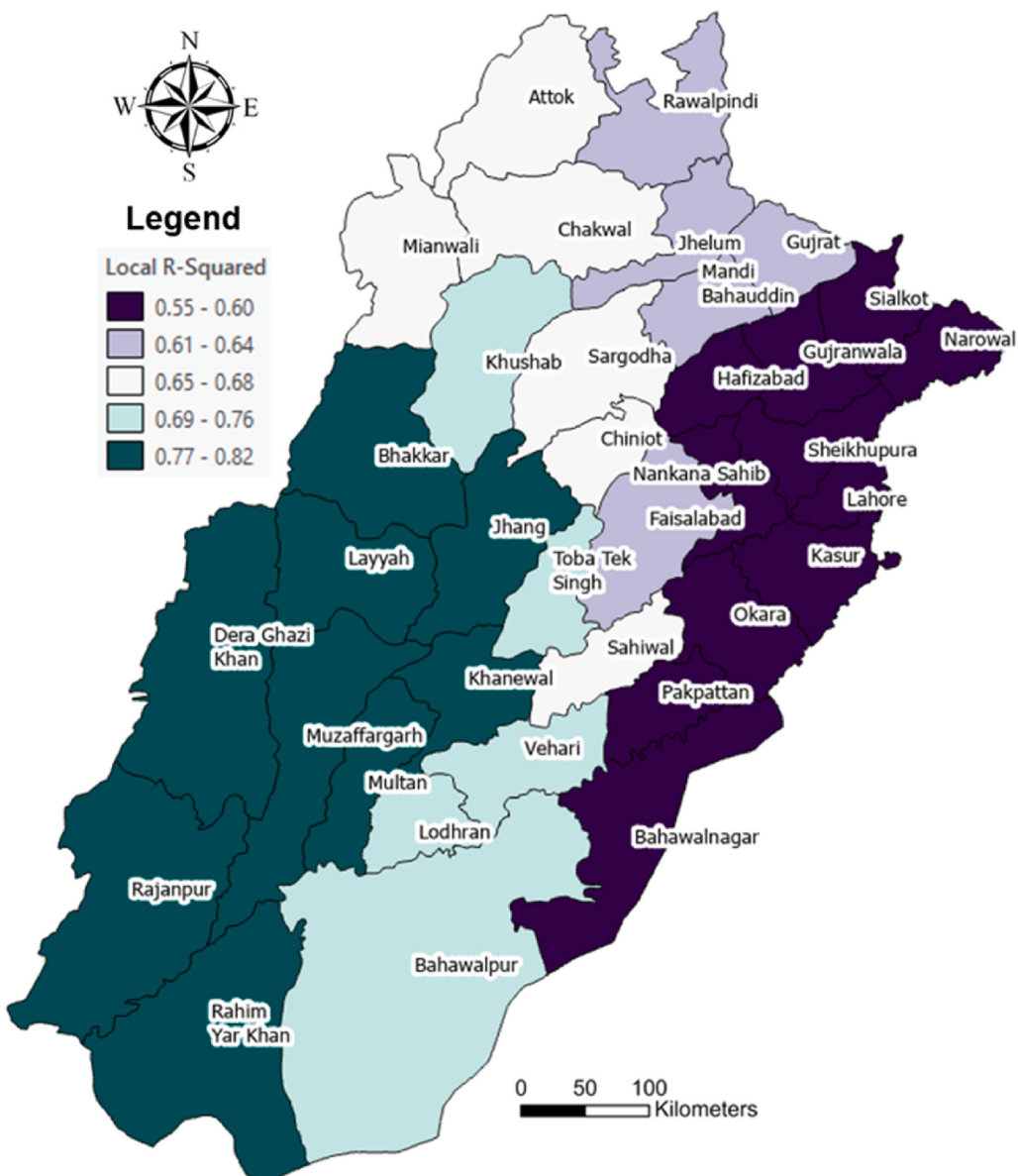


Fig. 10. Spatial distribution of Local R^2 values for the multivariate model to evaluate the association between LULC types and LST in the study area.

5. Conclusion

The present study utilizes remote sensing data to analyze the land use and land cover (LULC) changes along with assessing the spatial-temporal patterns and trends in the land surface temperature (LST) in Punjab, Pakistan—the most populous and developed province in Pakistan—during the past three decades (1990–2020). This is achieved through the integration of cloud computing-based platform (Google Earth Engine—GEE) and geospatial information models. In addition to exploring spatial heterogeneities, the potential association between LULC types and LST is evaluated, if any, using the geographically weighted regression. The results show an exponential increase in the urbanization-led built-up areas between the study period (~250% increase) with an annual increase of ~8.5%.

The largest contribution towards this built-up increase is due to the transition of rangelands (38%) and agriculture (37%) LULC to impervious surface. Noticeably, the highest percent increase in the built-up areas is observed in the most recent decade (i.e., 2010–2020)—showing the increasing pace of urbanization in the study area in recent years. Without proper planning, this rapid increase might create challenges hindering sustainable land management in Punjab. Similarly, the results on the LST show clear geographical disparities across the study area with south eastern, and western regions (mostly mountains, barren lands, and deserts) experiencing relatively higher LST as compared with northern areas. While statistically significant inter-decadal differences are ob-

served in the LST (99% confidence), the evaluation of top-20 cities in the study area in terms of population shows that the highest increase in LST during 1990–2020 is observed for Kasur (6 °C).

The produced maps in this study could provide useful references for informed strategies for not only the sustainability of land resource in the study area, but could also attribute towards reducing the UHI effect in rapidly urbanizing cities of the study area. The results presented here are of particular importance regarding establishing guidelines related to urban development (i.e., no net loss of green areas in regions with highest reduction in vegetation and rangelands). Similarly, city planners can prioritize the zones of the highest LST in the study area to formulate appropriate measures for cooling effect—enhancing the comfort level within built-up areas.

Through an application of remote sensing within the context of society and environment, this study put forth important insights related to LULC transitions in the study area, LST variations, and the geographical disparities in LST in response to LULC changes during past three decades. The results improve our understandings regarding LULC dynamics in the study area to support sustainable urbanization process. Furthermore, the LST evaluation and its association with LULC change progressively help informing adaptation related decisions and policy in Pakistan.

The authors do acknowledge the limitations of this current analysis despite its comprehensiveness regarding the subject matter. For example, the study at this stage only deals with the historical patterns and trends in LULC and LST. It would have been more useful if the future simulations of LULC and LST are produced to pinpoint the expected zones of larger transitions and higher temperature in the study area. These simulations could be produced using advance neural networks, machine learning, and artificial intelligence-based tools. However, this assessment in the study area at our scale of analysis requires higher computational capabilities—resulting in higher costs. Similarly, due to the large study area, there might be several localized patterns of LULC changes and LST. Also, LST variations at local levels would be sensitive to several other variables (i.e., wind circulations and building structures), which are not included in this study due to its scope. Hence, future work could consider our results to identify important areas for scaling-down the regions of interest to conduct these detailed assessments at local levels. Moreover, the association of LULC changes in this study is only focused on LST. This can be expanded to evaluate the influence of LULC change on several other phenomenon such as increase/decrease in exposure to natural hazards, land-degradation (i.e., soil erosion), carbon storage, and ecosystem service change among the many. This situation shows the broader implications of the current study and the LULC change and LST mapping.

Ethical statement

It is stated that all ethical practices have been followed in relation to the development, writing, and publication of the article.

CRediT authorship contribution statement

Mirza Waleed: Data curation, Formal analysis, Software, Writing – original draft, Writing – review & editing. **Muhammad Sajjad:** Conceptualization, Supervision, Project administration, Methodology, Visualization, Writing – original draft, Writing – review & editing.

Declaration of competing interest

The authors declare that they have no known competing financial interests or personal relationships that could have appeared to influence the work reported in this paper.

Acknowledgments

No specific funds were available to conduct this research. The first author is thankful to all the institutes (mentioned within the text) for the provisioning of relevant data to carry out this valuable study. The research is conducted in the absence of any commercial or financial relationships that could be construed as a potential conflict of interest. All the data used for several analyses are freely available and the resources are mentioned within the paper. The produced up-to-date LULC data are available upon request from the corresponding author for non-commercial research purposes.

Appendix A. Supplementary data

Supplementary data to this article can be found online at <https://doi.org/10.1016/j.rsase.2021.100665>.

References

- Abdullah, A.Y.M., Masrur, A., Adnan, M.S.G., Bakry, M.A.A., Hassan, Q.K., Dewan, A., 2019. Spatio-temporal patterns of land use/land cover change in the heterogeneous coastal region of Bangladesh between 1990 and 2017. *Rem. Sens.* 11 (7). <https://doi.org/10.3390/rs11070790>.
- Adnan, M.S.G., Abdullah, A.Y.M., Dewan, A., Hall, J.W., 2020. The effects of changing land use and flood hazard on poverty in coastal Bangladesh. *Land Use Pol.* 99. <https://doi.org/10.1016/j.landusepol.2020.104868>.
- Afrin, S., Gupta, A., Farjad, B., Ahmed, M.R., Achari, G., Hassan, Q., 2019. Development of land-use/land-cover maps using landsat-8 and MODIS data, and their integration for hydro-ecological applications. *Sensors* 19 (22), 4891. <https://doi.org/10.3390/s19224891>.
- Al-Rubkhi, A., Talal, A., Mohammed, A., 2017. Land use change analysis and modeling using open source (QGis)-Case study: boasher willayat. In: *Muscat: College of Arts and Social Science. Department of Geography, Sultan Qaboos University*.
- Alawamny, J.S., Balasundram, S.K., Mohd Hanif, A.H., Boon Sung, C.T., 2020. Detecting and analyzing land use and land cover changes in the region of Al-Jabal Al-Akhdar, Libya using time-series landsat data from 1985 to 2017. *Sustainability* 12 (11). <https://doi.org/10.3390/su12114490>.
- AlBeladi, A.A., Muqabil, A.H., 2018. Evaluating compressive sensing algorithms in through-the-wall radar via F1-score. *Int. J. Signal Imag. Syst. Eng.* 11 (3), 164–171.
- Amanollahi, J., Tzanis, C., Ramli, M., Abdullah, A., 2016. Urban heat evolution in a tropical area utilizing Landsat imagery. *Atmos. Res.* 167, 175–182. <https://doi.org/10.1016/j.atmosres.2016.07.003>

- 10.1016/j.atmosres.2015.07.019.
- Amir, S., Saqib, Z., Khan, A., Khan, M.I., Khan, M.A., Majid, A., 2019. Land cover mapping and crop phenology of Potohar region, Punjab, Pakistan. *Pakistan J. Agric. Sci.* 56 (1).
- Amiri, R., Weng, Q., Alimohammadi, A., Alavipanah, S.K., 2009. Spatial-temporal dynamics of land surface temperature in relation to fractional vegetation cover and land use/cover in the Tabriz urban area, Iran. *Rem. Sens. Environ.* 113 (12), 2606–2617.
- Arshad, A., Zhang, Z., Zhang, W., Dilawar, A., 2020. Mapping favorable groundwater potential recharge zones using a GIS-based analytical hierarchical process and probability frequency ratio model: a case study from an agro-urban region of Pakistan. *GeoSci. Front.* 11 (5), 1805–1819.
- Artis, D.A., Carnahan, W.H., 1982. Survey of emissivity variability in thermography of urban areas. *Rem. Sens. Environ.* 12 (4), 313–329.
- Attri, P., Chaudhry, S., Sharma, S., 2015. Remote sensing & GIS based approaches for LULC change detection—a review. *Int. J. Curr. Eng. Technol.* 5 (5), 3126–3137.
- Avdani, U., Jovanovska, G., 2016. Algorithm for automated mapping of land surface temperature using LANDSAT 8 satellite data. *J. Sens.* 1480307, 2016. <https://doi.org/10.1155/2016/1480307>.
- Borrelli, P., Robinson, D.A., Panagos, P., Lugato, E., Yang, J.E., Alewell, C., Wuepper, D., Montanarella, L., Ballabio, C., 2020. Land use and climate change impacts on global soil erosion by water (2015–2070). *Proc. Natl. Acad. Sci. Unit. States Am.* 117 (36), 21994–22001.
- Chachondhia, P., Shakya, A., Kumar, G., 2021. Performance evaluation of machine learning algorithms using optical and microwave data for LULC classification. *Rem. Sens. Appl.: Soc. Environ.* 100599. <https://doi.org/10.1016/j.rsase.2021.100599>.
- Chavez, P.S., 1988. An improved dark-object subtraction technique for atmospheric scattering correction of multispectral data. *Rem. Sens. Environ.* 24 (3), 459–479. [https://doi.org/10.1016/0034-4257\(88\)90019-3](https://doi.org/10.1016/0034-4257(88)90019-3).
- Cheema, M.J.M., Khaliq, T., Liaquat, M.U., Khan, M.M., Amin, H., 2020. Quantification of land use changes in complex cropping of irrigated Indus basin, Pakistan using MODIS vegetation time series data. *Pakistan J. Agric. Sci.* 57 (2).
- Chen, D., Lu, X., Liu, X., Wang, X., 2019. Measurement of the eco-environmental effects of urban sprawl: theoretical mechanism and spatiotemporal differentiation. *Ecol. Indicat.* 105, 6–15.
- da Cunha, E.R., Santos, C.A.G., da Silva, R.M., Bacani, V.M., Pott, A., 2021. Future scenarios based on a CA-Markov land use and land cover simulation model for a tropical humid basin in the Cerrado/Atlantic forest ecotone of Brazil. *Land Use Pol.* 101, 105141.
- Das, S., Angadi, D.P., 2020. Land use-land cover (LULC) transformation and its relation with land surface temperature changes: a case study of Barrackpore Subdivision, West Bengal, India. *Rem. Sens. Appl.: Soc. Environ.* 19, 100322. <https://doi.org/10.1016/j.rsase.2020.100322>.
- Dewan, A., Kiselev, G., Botje, D., Mahmud, G.I., Bhuiyan, M.H., Hassan, Q.K., 2021a. Surface urban heat island intensity in five major cities of Bangladesh: patterns, drivers and trends. *Sustain. Cities Soc.* 71. <https://doi.org/10.1016/j.scs.2021.102926>.
- Dewan, A., Kiselev, G., Botje, D., Mahmud, G.I., Bhuiyan, M.H., Hassan, Q.K., 2021b. Surface urban heat island intensity in five major cities of Bangladesh: patterns, drivers and trends. *Sustain. Cities Soc.* 71, 102926. <https://doi.org/10.1016/j.scs.2021.102926>.
- Dimarco, A., Chen, B., Trisurat, Y., Tuankrua, V., Arshad, A., Hussain, Y., Measho, S., Guo, L., Kayiranga, A., Zhang, H., 2021. Spatiotemporal shifts in thermal climate in responses to urban cover changes: a-case analysis of major cities in Punjab, Pakistan. *Geomatics, Nat. Hazards Risk* 12 (1), 763–793.
- Ejiajagh, I.R., Ahmed, M.R., Hassan, Q.K., Dewan, A., Gupta, A., Rangelova, E., 2020. Use of remote sensing in comprehending the influence of urban landscape's composition and configuration on land surface temperature at neighbourhood scale. *Rem. Sens.* 12 (15), 2508.
- Gorelick, N., Hancher, M., Dixon, M., Ilyushchenko, S., Thau, D., Moore, R., 2017. Google earth engine: planetary-scale geospatial analysis for everyone. *Rem. Sens. Environ.* 202, 18–27. <https://doi.org/10.1016/j.rse.2017.06.031>.
- Gumma, M.K., Thenkabail, P.S., Teluguntla, P.G., Oliphant, A., Xiong, J., Giri, C., Pyla, V., Dixit, S., Whitbread, A.M., 2020. Agricultural cropland extent and areas of South Asia derived using Landsat satellite 30-m time-series big-data using random forest machine learning algorithms on the Google Earth Engine cloud. *GIScience Remote Sens.* 57 (3), 302–322.
- Gunawardena, K.R., Wells, M.J., Kershaw, T., 2017. Utilising green and bluespace to mitigate urban heat island intensity. *Sci. Total Environ.* 584, 1040–1055.
- Han, J., 2020. Can urban sprawl be the cause of environmental deterioration? Based on the provincial panel data in China. *Environ. Res.* 189, 109954.
- Hassan, Z., Shabbir, R., Ahmad, S.S., Malik, A.H., Aziz, N., Butt, A., Erum, S., 2016. Dynamics of land use and land cover change (LULCC) using geospatial techniques: a case study of Islamabad Pakistan. *SpringerPlus* 5 (1), 812. <https://doi.org/10.1186/s40064-016-2414-z>.
- Hislop, S., Jones, S., Soto-Berelov, M., Skidmore, A., Haywood, A., Nguyen, T.H., 2018. Using landsat spectral indices in time-series to assess wildfire disturbance and recovery. *Rem. Sens.* 10 (3), 460.
- Hong, C., Burney, J.A., Pongrayz, J., Nabel, J., Mueller, N.D., Jackson, R.B., Davis, S.J., 2021. Global and regional drivers of land-use emissions in 1961–2017. *Nature* 589 (7843), 554–561. <https://doi.org/10.1038/s41586-020-03138-y>.
- Hu, Y., Batunacun, Zhen, L., Zhuang, D., 2019. Assessment of land-use and land-cover change in Guangxi, China. *Sci. Rep.* 9 (1), 2189. <https://doi.org/10.1038/s41598-019-38487-w>.
- Huete, A., Didan, K., Miura, T., Rodriguez, E.P., Gao, X., Ferreira, L.G., 2002. Overview of the radiometric and biophysical performance of the MODIS vegetation indices. *Rem. Sens. Environ.* 83 (1), 195–213. [https://doi.org/10.1016/S0034-4257\(02\)00096-2](https://doi.org/10.1016/S0034-4257(02)00096-2).
- Huete, A.R., 1988. A soil-adjusted vegetation index (SAVI). *Rem. Sens. Environ.* 25 (3), 295–309.
- Huq, S., 2001. Climate change and Bangladesh. *Science* 294 (5547), 1617–1618.
- Hussain, S., Karuppannan, S., 2021. Land use/land cover changes and their impact on land surface temperature using remote sensing technique in district Khanewal, Punjab Pakistan. *Geol. Ecol. Landsc.* 1–13.
- Hussain, S., Mubeen, M., Ahmad, A., Akram, W., Hammad, H.M., Ali, M., Masood, N., Amin, A., Farid, H.U., Sultana, S.R., 2019. Using GIS tools to detect the land use/land cover changes during forty years in Lodhran district of Pakistan. *Environ. Sci. Pollut. Control Ser.* 1–17.
- Hussein, K., Alkaabi, K., Ghebreyesus, D., Liaquat, M.U., Sharif, H.O., 2020. Land use/land cover change along the Eastern Coast of the UAE and its impact on flooding risk. *Geomatics, Nat. Hazards Risk* 11 (1), 112–130.
- Ihlen, V., 2019. Landsat 8 Data Users Handbook. US Geological Survey: Sioux Falls, SD, USA.
- Imran, H., Hossain, A., Islam, A.S., Rahman, A., Bhuiyan, M.A.E., Paul, S., Alam, A., 2021a. Impact of land cover changes on land surface temperature and human thermal comfort in Dhaka city of Bangladesh. *Earth Syst. Environ.* 1–27.
- Imran, H.M., Hossain, A., Islam, A.K.M.S., Rahman, A., Bhuiyan, M.A.E., Paul, S., Alam, A., 2021b. Impact of land cover changes on land surface temperature and human thermal comfort in Dhaka city of Bangladesh. *Earth Syst. Environ.* 5 (3), 667–693. <https://doi.org/10.1007/s41748-021-00243-4>.
- Imran, M., Sumra, K., Abbas, N., Majeed, I., 2019. Spatial distribution and opportunity mapping: applicability of evidence-based policy implications in Punjab using remote sensing and global products. *Sustain. Cities Soc.* 50, 101652.
- Islam, K., Jashimuddin, M., Nath, B., Nath, T.K., 2018. Land use classification and change detection by using multi-temporal remotely sensed imagery: the case of Chunati wildlife sanctuary, Bangladesh. *Egypt. J. Rem. Sens. Space Sci.* 21 (1), 37–47.
- Jarchow, C.J., Didan, K., Barreto-Muñoz, A., Nagler, P.L., Glenn, E.P., 2018. Application and comparison of the MODIS-derived enhanced vegetation index to VIIRS, landsat 5 TM and landsat 8 OLI platforms: a case study in the arid Colorado river delta, Mexico. *Sensors* 18 (5), 1546.
- Jung, J., Maeda, M., Chang, A., Bhandari, M., Ashpare, A., Landivar-Bowles, J., 2021. The potential of remote sensing and artificial intelligence as tools to improve the resilience of agriculture production systems. *Curr. Opin. Biotechnol.* 70, 15–22.
- Kalnay, E., Cai, M., 2003. Impact of urbanization and land-use change on climate. *Nature* 423 (6939), 528–531. <https://doi.org/10.1038/nature01675>.
- Karimi, A., Pahlavani, P., Bigdeli, B., 2017. Land use analysis ON land surface temperature IN urban areas using a geographically weighted regression and landsat 8 imagery, a case study: tehran, Iran. *Int. Arch. Photogram. Rem. Sens. Spatial Inf. Sci.* XLII-4/W4 XLII-4/W4, 117–122. <https://doi.org/10.5194/isprs-archives-XLII-4-W4-117-2017>.
- Khana, M.M., Cheemab, M.J.M., Mahmood, T., Hussain, S., Waqase, M.S., Nauman, H.M., Nawaza, M., Saifullah, M., 2020. Crop area mapping by intelligent pixel information inferred using 250m modis vegetation timeseries in transboundary indus basin. *Big Data Water Resour. Eng. (BDWRE)* 1 (2), 31, 32–35Volume.
- Kumar, L., Mutanga, O., 2018. Google earth engine applications since inception: usage, trends, and potential. *Rem. Sens.* 10 (10). <https://doi.org/10.3390/rs10101509>.
- Kundu, D., Pandey, A.K., 2020. World urbanisation: trends and patterns. In: Kundu, D., Sietchiping, R., Kinyanjui, M. (Eds.), *Developing National Urban Policies: Ways Forward to Green and Smart Cities*. Springer Singapore, pp. 13–49. https://doi.org/10.1007/978-981-15-3738-7_2.

- Li, Q., Qiu, C., Ma, L., Schmitt, M., Zhu, X., 2020. Mapping the land cover of Africa at 10 m resolution from multi-source remote sensing data with Google earth engine. *Rem. Sens.* 12 (4). <https://doi.org/10.3390/rs12040602>.
- Magliocca, N.R., Rudel, T.K., Verburg, P.H., McConnell, W.J., Mertz, O., Gerstner, K., Heinemann, A., Ellis, E.C., 2015. Synthesis in land change science: methodological patterns, challenges, and guidelines. *Reg. Environ. Change* 15 (2), 211–226.
- Majeed, M., Tariq, A., Anwar, M.M., Khan, A.M., Arshad, F., Mumtaz, F., Farhan, M., Zhang, L., Zafar, A., Aziz, M., 2021. Monitoring of land use–land cover change and potential causal factors of climate change in Jhelum district, Punjab, Pakistan, through GIS and multi-temporal satellite data. *Land* 10 (10), 1026.
- Moretti, E., 2014. Cities and Growth. International Growth Center.
- Ogunjobi, K.O., Adamu, Y., Akinsanola, A.A., Orimoloye, I.R., 2018. Spatio-temporal analysis of land use dynamics and its potential indications on land surface temperature in Sokoto Metropolis, Nigeria. *Roy. Soc. Open Sci.* 5 (12), 180661. <https://doi.org/10.1098/rsos.180661>.
- Osgouei, P.E., Kaye, S., 2017. Analysis of land cover/use changes using Landsat 5 TM data and indices. *Environ. Monit. Assess.* 189 (4), 136.
- Özelkan, E., 2020. Water body detection analysis using NDWI indices derived from landsat-8 OLI. *Pol. J. Environ. Stud.* 29 (2), 1759–1769.
- Pramanik, S., Punia, M., 2020. Land use/land cover change and surface urban heat island intensity: source–sink landscape-based study in Delhi, India. *Environ. Dev. Sustain.* 22 (8), 7331–7356.
- Qi, Y., Wu, J., Li, J., Yu, Y., Peng, F., Sun, C., 2013. Landscape dynamics of medium-and small-sized cities in eastern and western China: a comparative study of pattern and driving forces. *Shengtai Xuebao/Acta Ecologica Sinica* 33 (1), 275–285.
- Qu, L.a., Chen, Z., Li, M., Zhi, J., Wang, H., 2021. Accuracy improvements to pixel-based and object-based lulc classification with auxiliary datasets from Google Earth engine. *Rem. Sens.* 13 (3), 453.
- Quan, J., Zhan, W., Chen, Y., Wang, M., Wang, J., 2016. Time series decomposition of remotely sensed land surface temperature and investigation of trends and seasonal variations in surface urban heat islands. *J. Geophys. Res.: Atmosphere* 121 (6), 2638–2657.
- Rahman, M., Ningsheng, C., Mahmud, G.I., Islam, M.M., Pourghasemi, H.R., Ahmad, H., Habumugisha, J.M., Washakh, R.M.A., Alam, M., Liu, E., Han, Z., Ni, H., Shufeng, T., Dewan, A., 2021. Flooding and its relationship with land cover change, population growth, and road density. *GeoSci. Front.* 12 (6), 101224. <https://doi.org/10.1016/j.gsf.2021.101224>.
- Ren, C., Ng, E.Y.y., Katzschnier, L., 2011. Urban climatic map studies: a review. *Int. J. Climatol.* 31 (15), 2213–2233.
- Rosina, K., Batista e Silva, F., Vizcaino, P., Marín Herrera, M., Freire, S., Schiavina, M., 2020. Increasing the detail of European land use/cover data by combining heterogeneous data sets. *Int. J. Digit. Earth* 13 (5), 602–626. <https://doi.org/10.1080/17538947.2018.1550119>.
- Rouse, J.W., Haas, R.H., Schell, J.A., Deering, D.W., 1974. Monitoring Vegetation Systems in the Great Plains with ERTS, vol. 351. NASA special publication, p. 309.
- Rosenstein, O., Qin, Z., Derimian, Y., Karnieli, A., 2014. Derivation of land surface temperature for Landsat-8 TIRS using a split window algorithm. *Sensors* 14 (4), 5768–5780.
- Saha, S., Saha, A., Das, M., Saha, A., Sarkar, R., Das, A., 2021. Analyzing spatial relationship between land use/land cover (LULC) and land surface temperature (LST) of three urban agglomerations (UAs) of Eastern India. *Rem. Sens. Appl.: Soc. Environ.* 22, 100507. <https://doi.org/10.1016/j.rsase.2021.100507>.
- Sajjad, M., 2021. Disaster resilience in Pakistan: a comprehensive multi-dimensional spatial profiling. *Appl. Geogr.* 126, 102367. <https://doi.org/10.1016/j.apgeog.2020.102367>.
- Saleem, M.S., Ahmad, S.R., Shafiq Ur, R., Javed, M.A., 2020. Impact assessment of urban development patterns on land surface temperature by using remote sensing techniques: a case study of Lahore, Faisalabad and Multan district. *Environ. Sci. Pollut. Control Ser.* 27 (32), 39865–39878. <https://doi.org/10.1007/s11356-020-10050-5>.
- Saputra, M.H., Lee, H.S., 2019. Prediction of land use and land cover changes for north sumatra, Indonesia, using an artificial-neural-network-based cellular automaton. *Sustainability* 11 (11). <https://doi.org/10.3390/su11113024>.
- Sarkodie, S.A., Owusu, P.A., Leirvik, T., 2020. Global effect of urban sprawl, industrialization, trade and economic development on carbon dioxide emissions. *Environ. Res. Lett.* 15 (3), 034049.
- Shah, A., Ali, K., Nizami, S.M., 2021. Four decadal urban land degradation in Pakistan a case study of capital city Islamabad during 1979–2019. *Environ. Sustain. Indic.* 10, 100108. <https://doi.org/10.1016/j.indic.2021.100108>.
- Shelestov, A., Lavreniuk, M., Kussul, N., Novikov, A., Skakun, S., 2017. Exploring Google Earth Engine platform for big data processing: classification of multi-temporal satellite imagery for crop mapping. *Front. Earth Sci.* 5, 17.
- Siddiqui, S., Javid, K., 2019. Spatio-temporal analysis of aridity over Punjab Province, Pakistan using remote sensing techniques. *Int. J. Econ. Environ. Geol.* 1–10.
- Simwanda, M., Ranagalage, M., Estoque, R.C., Murayama, Y., 2019. Spatial analysis of surface urban heat islands in four rapidly growing African cities. *Rem. Sens.* 11 (14), 1645.
- Song, X.-P., Hansen, M.C., Stehman, S.V., Potapov, P.V., Tyukavina, A., Vermote, E.F., Townshend, J.R., 2018a. Global land change from 1982 to 2016. *Nature* 560 (7720), 639–643.
- Song, X.P., Hansen, M.C., Stehman, S.V., Potapov, P.V., Tyukavina, A., Vermote, E.F., Townshend, J.R., 2018b. Global land change from 1982 to 2016. *Nature* 560 (7720), 639–643. <https://doi.org/10.1038/s41586-018-0411-9>.
- Statistics, P. B. o., 2017. Population Census, 2017.
- Talukdar, S., Singha, P., Mahato, S., Shahfahad Pal, S., Liou, Y.-A., Rahman, A., 2020. Land-use land-cover classification by machine learning classifiers for satellite observations—a review. *Rem. Sens.* 12 (7). <https://doi.org/10.3390/rs12071135>.
- Ullah, Tahir, Akbar, Hassan, Dewan, Khan, Khan, 2019. Remote sensing-based quantification of the relationships between land use land cover changes and surface temperature over the lower himalayan region. *Sustainability* 11 (19). <https://doi.org/10.3390/su11195492>.
- Vinayak, B., Lee, H.S., Gedem, S., 2021. Prediction of land use and land cover changes in Mumbai city, India, using remote sensing data and a multilayer perceptron neural network-based Markov chain model. *Sustainability* 13 (2). <https://doi.org/10.3390/su13020471>.
- Wang, L., Diao, C., Xian, G., Yin, D., Lu, Y., Zou, S., Erickson, T.A., 2020. A Summary of the Special Issue on Remote Sensing of Land Change Science with Google Earth Engine. Elsevier.
- Wang, Y., Berardi, U., Akbari, H., 2016. Comparing the effects of urban heat island mitigation strategies for Toronto, Canada. *Energy Build.* 114, 2–19.
- Winkler, K., Fuchs, R., Rounsevell, M., Herold, M., 2021. Global land use changes are four times greater than previously estimated. *Nat. Commun.* 12 (1), 2501. <https://doi.org/10.1038/s41467-021-22702-2>.
- Xiong, J., Thenkabail, P.S., Gumma, M.K., Teluguntla, P., Poehnelt, J., Congalton, R.G., Yadav, K., Thau, D., 2017. Automated cropland mapping of continental Africa using Google Earth Engine cloud computing. *ISPRS J. Photogrammetry Remote Sens.* 126, 225–244.
- Xu, H., 2006. Modification of normalised difference water index (NDWI) to enhance open water features in remotely sensed imagery. *Int. J. Rem. Sens.* 27 (14), 3025–3033.
- Xue, J., Su, B., 2017. Significant remote sensing vegetation indices: a review of developments and applications. *J. Sensors* 2017, 1353691. <https://doi.org/10.1155/2017/1353691>.
- Yin, G., Mariethoz, G., McCabe, M.F., 2017. Gap-filling of landsat 7 imagery using the direct sampling method. *Rem. Sens.* 9 (1), 12.
- Yohannes, H., Soromessa, T., Argaw, M., Dewan, A., 2021. Impact of Landscape Pattern Changes on Hydrological Ecosystem Services in the Beressa Watershed of the Blue Nile Basin in Ethiopia. *Science of The Total Environment*, p. 148559.
- Zha, Y., Gao, J., Ni, S., 2003. Use of normalized difference built-up index in automatically mapping urban areas from TM imagery. *Int. J. Rem. Sens.* 24 (3), 583–594.
- Zhang, H.K., Roy, D.P., Yan, L., Li, Z., Huang, H., Vermote, E., Skakun, S., Roger, J.-C., 2018. Characterization of Sentinel-2A and Landsat-8 top of atmosphere, surface, and nadir BRDF adjusted reflectance and NDVI differences. *Rem. Sens. Environ.* 215, 482–494.
- Zope, P.E., Eldho, T.I., Jothiprakash, V., 2016. Impacts of land use–land cover change and urbanization on flooding: a case study of Oshiwara River Basin in Mumbai, India. *Catena* 145, 142–154. <https://doi.org/10.1016/j.catena.2016.06.009>.
- Zurqani, H.A., Post, C.J., Mikhailova, E.A., Schlautman, M.A., Sharp, J.L., 2018. Geospatial analysis of land use change in the savannah river basin using Google earth engine. *Int. J. Appl. Earth Obs. Geoinf.* 69, 175–185.